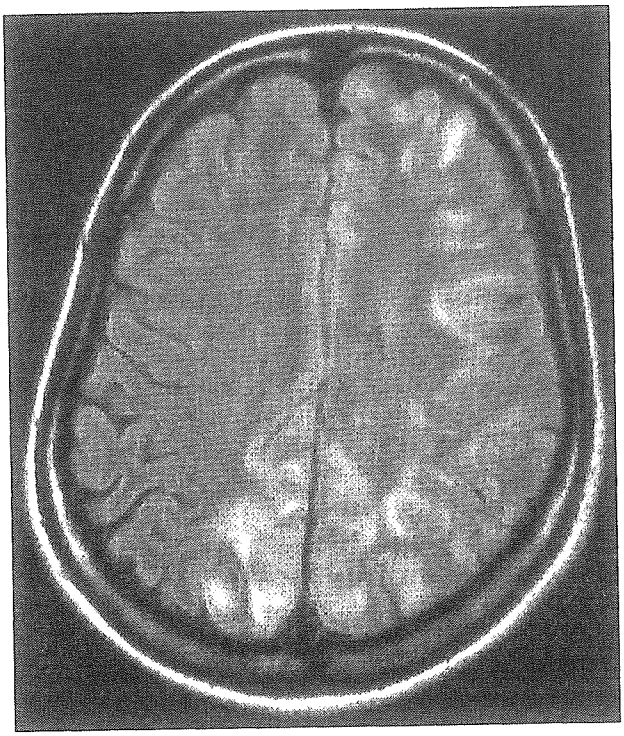

Figure 1 Fluid-attenuated inversion recovery (FLAIR) image showing parietal and occipital, but also some typical frontal lobe edema. (Case 1)

necessity to perform routine MR scanning on all severe preeclampsia patients. However, patients who show elevated diastolic blood pressure and liver enzymes should be recognized as possible candidates for eclampsia, even though appropriate treatments may already have been implemented. Emergency cesarian section prevented five women from developing eclampsia, according to their abnormal MR images. In the remaining six women, delivery may have been delayed too long because magnesium sulfate and emergency cesarian sections could not prevent these women from developing eclampsia.

From our data, we conclude that cerebral damage can occur without obvious symptoms in a number of severe preeclamptic women prior to developing eclampsia. Elevated diastolic blood pressure and liver enzymes, especially serum AST, may be predictive parameters. Frequent routine evaluations of clinical parameters are very important and earlier deliveries are highly recommended in severe preeclampsia cases before brain damage begins.

When prolonged hypertension and elevated liver enzymes are observed postpartum in such patients, MR scanning is recommended because medication differs according to the diffusion weighted images. In vasogenic edema, lowering blood pressure is necessary, while in cytotoxic edema, stabilizing blood pressure is recommended even if blood pressure is rather high. MR scanning during pregnancy due to severe preeclampsia might be useful in a limited number of situations when, in the second trimester, the pregnancy is being continued in a maternal intensive care unit until fetal maturation. Even with such a delayed delivery policy, emergency cesarian section may be inevitable when abnormal MR images are obtained.

Brain MR scanning is now used widely in various fields of clinical medicine. Peterkin et al. [14] documented eclampsia exhibiting peculiar MR images in 1992, and Brown et al. [4] reported abnormal brain radiological findings within computed tomography in 1988. In 1997, Morris et al. [12] and colleagues confirmed remarkable changes in the area of the posterior cerebral arteries in eclampsia after Hinchey et al. [8] identified reversible posterior leukoenchephalopathy syndrome for a partic-

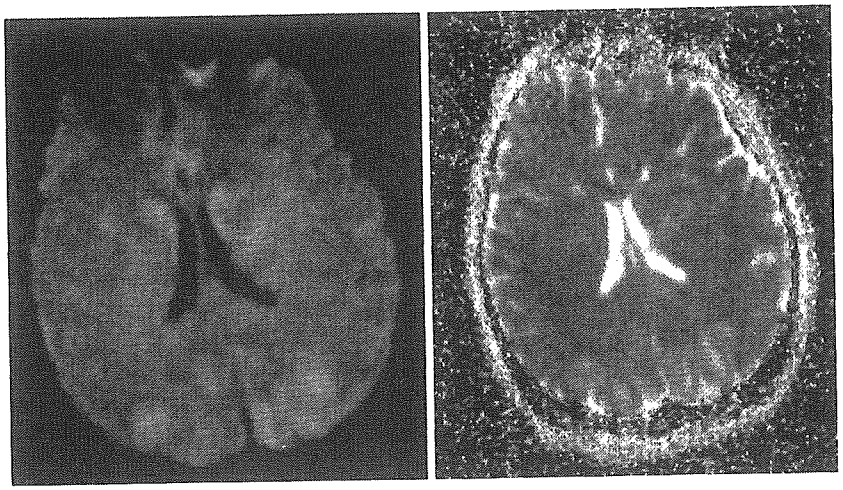

Figure 2 Vasogenic edema in posterior lobe. Right: Diffusion-weithted (DW) image (b-value: 1000 s/mm^2). Left: Apparent diffusion coefficient (ADC) map. (Case 8)

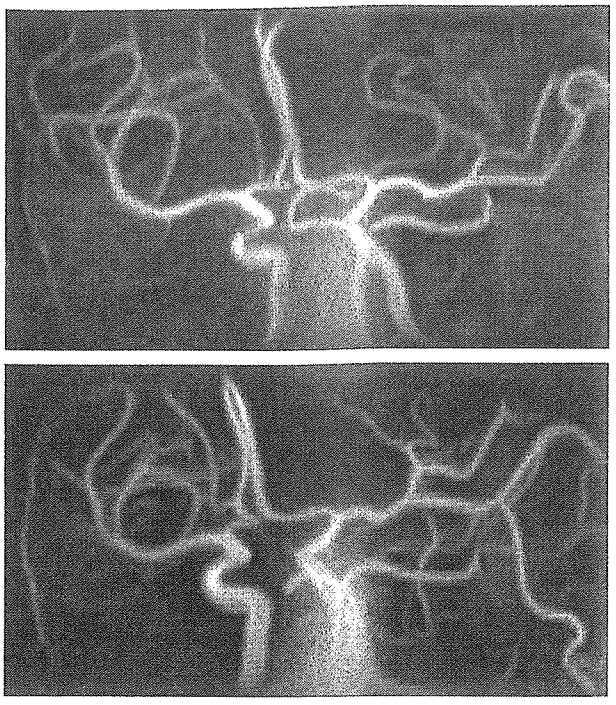

Figure 3 Above: Three-dimensional time-of-flight MR angiography (3D-TOF-MRA) showing vasoconstriction in right carotid artery. Below: Vasoconstriction was disappeared in 11 days. (Case 4)

ular type of brain edema in 1996. Thus, the cause of eclampsia is today believed to be cerebral edema. Cunningham and Twickler [6] thought that cerebral change is related to both ischemic (cytotoxic) and hyperperfusion (vasogenic) edema; conversely, Apollon et al. [2] used single-photon-emission computed tomography and provided evidence for hyperperfusion and vasogenic (hydrostatic) edema.

Using transcranial Doppler ultrasound, Williams and Wilson [19] determined that, in preeclampsia, increased cerebral perfusion pressure counterbalanced by increased cerebralovascular resistance is associated with no net change in cerebral blood flow. They concluded that loss of auto-regulation of cerebral blood flow manifesting as decreased vascular resistance eventually results in cerebral perfusion in eclampsia similar to that seen in hypertensive encephalopathy unrelated to pregnancy. Brackley et al. [3] showed that cerebral vasospasm in preeclamptic patients increased cerebral arterial wall stiffness and vasoconstriction. Rutherford et al. [15] reported that narrowing of cerebral vessels detectable on MR angiography does not occur commonly in preeclampsia, and MR spectroscopy results suggest that there is a relatively greater incidence of cerebral ischemia in preeclampsia cases than in normal pregnancy. Our data also suggested that 3D-TOF-MRA had less sensitivity and specificity than reported transcranial Doppler ultrasound. It is possible that cerebral change could already exist in preeclampsia cases and that preeclamptic women who have suffered a transient loss of cerebral vascular auto-regulation develop eclampsia.

Table 2 Prediction of eclampsia with MRI diagnoses.

	Eclampsia	Non-eclampsia
abnormal MRI	6	5
normal MRI	0	30

Sensitivity of 100.0%, specificity of 85.7%, positive predictive value of 54.5%, negative predictive value of 100.0%, and prediction accuracy of 87.8%. P=0.00001.

We hypothesized that abnormal cerebral MR images predict the onset of eclampsia in severe preeclamptic women. In our study 6 of 11 cases developed eclampsia, supporting this hypothesis, we believe the accumulation of cerebral damage can eventually result in lost hemodynamic auto-regulation and become visible in MR images in severe eclampsia cases as cerebral edema in particular, but not vasoconstriction. All six eclamptic women in our study had cerebral edema; however, from our small data sample it is impossible to suggest that severe preeclamptic women without abnormal MR images would not develop eclampsia. Although Cunningham et al. [6] reported a study in which only 10 of 175 eclamptic women demonstrated cerebral edema, it is thought that techanical progress may reveal visible cerebral damage in eclampsia.

Schwartz [17] showed that abnormal red blood cell morphology and serum LDH (lactic dehydrogenese) levels indicate cerebral edema in MR images, and blood pressure has no significant influence. Our results suggest that diastolic blood pressure and serum AST have considerable influence, while LDH does not. Today, diastolic blood pressure is accepted generally as a category of severity of preeclampsia, and serum AST is regarded as a diagnostic variable in HELLP syndrome. Jurgensen [9] reported a case of postpartum blindness caused by brain edema due to HELLP syndrome. In the present study, serum AST levels were derived as a variable in obtaining abnormal MR images, suggesting a relationship between parenchymal liver damage and brain edema. Cunningham et al. [5] described elevated serum AST levels in blindness associated with severe preeclampsia and eclampsia. Porostaglandins, nitric oxide, enodoterienes, vascular endotherial growth factors, genetic predisposition, immunological factors, inflammatory factors, etc, could have an important role in the severity of preeclampsia, but they are not easily accessed clinically. These patho-physiological tests are able to detect severe preeclampsia in pregnant women, but are no easily accessible marker to predict eclampsia when severe preeclampsia has not yet been established.

Antunes et al. [1] reported that radiological lesions compatible with transient white matter edema evolved

Table 3 Clinical parameters in eclampsia and non-eclampsia.

	Non-eclampsia (n=35)	Eclampsia (n=6)	P-value
serum ALT (IU/L)	19.2±3.24	95.4±41.1	0.0001*
serum LDH (IU/L)	289.0±19.0	738.0±327.7	0.0016*
serum AST (IU/L)	39.2±15.04	153.0±68.4	0.0143*
serum Creatinine (mg/dl)	0.6±0.02	0.81±0.13	0.0159*
Diastolic BP (mmHg)	104.2±2.44	114.4±3.39	0.0412*
Hematocrit (%)	34.3±1.42	36.3±2.78	0.0643
Systolic BP (mmHg)	175.2±2.76	182.7±3.40	0.14
Age (years old)	30.8±0.6	33.1±1.8	0.18
serum UA (mg/dl)	6.06±0.31	6.67±0.99	0.19
Body Mass Index (kg/m²)	26.4±1.02	24.3±0.54	0.19
AT-3 (%)	90.9±3.20	80.0±5.87	0.23
D-dimer (mg/mL)	3.78±0.63	6.51±2.56	0.322
Platelet (×109/L)	200.4±1.3	183.7±3.7	0.37
urine Protein (g/day)	2.8±0.53	5.0±3.53	0.43
BUN (mg/dl)	10.9±1.03	13.3±2.90	0.48
GFR (mL/min)	109.1±6.2	97.2±15.2	0.51
serum Albumin (g/dl)	2.95±0.07	3.17±0.13	0.53
FDP (mg/mL)	8.1±1.06	10.1±2.76	0.58
serum Ca (mg/dl)	8.46±0.23	8.35±0.45	0.74
Fetal Body Weight (g)	2189.2±170.5	2228.3±189.1	0.81

* means statistical significant in Bonferroni test.

Table 4 Clinical parameters in abnormal MRI and normal MRI.

	Normal MRI (n=30)	Abnormal MRI (n=11)	P-value
Diastolic BP (mmHg)	102±2.0	114.0±2.0	0.0007*
sAST (IU/L)	25.0±3.0	138.1±56.1	0.0039*
sALT (IU/L)	21.0±4.1	56.3±26.1	0.0442*
sLDH (IU/L)	289±21.0	534±186.2	0.06
Hematocrit (%)	33.3±1.42	35.3±1.41	0.16
Systolic BP (mmHg)	174.2±2.72	180.2±3.41	0.16
Creatinine (mg/dl)	0.6±0.02	0.7±0.13	0.21
Age (years old)	30.8±1.41	32.1±1.33	0.88
U. Protein (g/day)	2.55±0.52	4.78±1.90	0.31
sCa (mg/dl)	8.4±0.22	8.4±0.31	0.35
D-dimer (mg/mL)	3.7±0.50	5.6±1.72	0.4
Platelet (×109/L)	200.4±1.31	223.7±2.42	0.46
UA (mg/dl)	6.2±0.21	7.4±0.99	0.73
sAlbumin (g/dl)	2.95±0.09	3.17±0.09	0.75
BUN (mg/dl)	11.9±1.03	12.3±2.40	0.78
AT-3 (%)	89.9±3.40	88.0±5.87	0.79
Fetal Body Weight (g)	2188.2±171.6	2230.3±199.2	0.80
GFR (mL/min)	118.1±7.2	105.2±10.2	0.84
Body Mass Index (kg/m²)	26.4±1.02	26.3±1.04	0.86
FDP (mg/mL)	8.1±1.06	8.1±1.16	0.92

* means statistical signifficant in Bonferroni test.

Table 5 Prediction of abnormal MRI by stepwise discriminant analysis using diastolic BP and AST.

	Expected abnormal MRI	Expected normal MRI
true abnormal MRI	5	6
true normal MRI	1	29

Prediction accuracy of 82.9% was calculated. P=0.0007.

into leukomalacia, and Shwartz et al. [17] reported that posterior leukoencephalopathy is not always reversible. These reports concluded that immediate and appropriate treatment should be started. Garg et al. [7] emphasized that early recognition of posterior leukoencephalopathy is of paramount importance, as the prompt control of blood pressure can bring about a reversal of the syndrome. Delay in diagnosis and treatment can result in permanent damage to brain tissues. Schaefer et al. [16]

Table 6 Intervals of MRI scannings until the loss of abnormal images.

Case	MRI	Loss of abnormal findings	vasoconstriction	Loss of abnormal findings	Scanning (times)
1	multi-lobal vasogenic edema, minimal infarction	<12 days	left ACA (*suspected)	<380 days	6
2	posterior leukoencephalopathy	<15 days	(−)		2
3	basal ganglia vasogenic edema	<20 days	(−)		2
4	multi-lobal edema	<15 days	right CA	<12 days	2
5	(−)		right MCA (*suspected)	<132 days	2
6	multi-lobal vasogenic edema, minimal infarction	<92 days	(−)		3
7	temporal and posterior leukoencephalopathy	<30 days	(−)		2
8	posterior encephalopathy	<68 days	(−)		4
9	multi-lobal edema	<7 days	(−)		2
10	(−)		blt. ACA/PCA	<10 days	1
11	basal ganglia vasogenic edema	<30 days	(−)		2

ACA: anterior cerebral artery, CA: carotid artery, MCA: mid cerebral artery. *suspected: no denial of anatomical variation.

reported that diffusion-weighted imaging (DWI) could differentiate between vasogenic edema and cytotoxic edema, as well as between hypertensive encephalopathy and infarction, two different entities with different treatment protocols. They also emphasized that DWI should be performed on all eclamptic women as part of their evaluation.

It is thought that, as Rutherford et al. [15] concluded, MRI is not clinically cost-effective when used routinely in preeclampsia screening. However, MR scanning is to be recommended when a delayed delivery is chosen when fetal maturation in severe preeclampsia cases is desired, especially when the patient exhibits elevated diastolic blood pressure and elevated liver enzymes. In eclampsia cases, MR scanning is very useful and should be repeated until cerebral edema has disappeared.

References

[1] Antunes NL, TN Small, D George, F Boulad, E Lis: Posterior leukoencephalopathy syndrome may not be reversible. Pediatr Neurol 20(3) (1999 Mar) 241

[2] Apollon KM, JN Robinson, RB Schwartz, ER Norwitz: Cortical blindness in severe preeclampsia: Computed tomoguraphy, magnetic resonance imaging, and single-photon-emission computed tomography findings. Obstet Gynecol 95 (2000) 1017

[3] Brackley KJ, MM Ramsay, FB Pipkin, PC Rubin: The maternal cerebral circulation in preeclampsia: Investigations using Laplace transform analysis of Doppler waveforms. Br J Obstet Gynecol 107 (2000) 492

[4] Brown CEL, PD Purdy, FG Cunningham: Head computed tomographic scans in women with eclampsia. Am J Obstet Gynecol 159 (1988a) 915

[5] Cunningham FG, CO Fernandez, C Hernandez: Blindness associated with preeclampsia and eclampsia. Am J Obstet Gynecol 172 (1995) 1291

[6] Cunningham FG, D Twickler: Cerebral edema complicating eclampsia. Am J Obstet Gynecol 182 (2000) 94

[7] Garg RK: Posteriior leukoencephalopathy syndrome. Postgrad Med J 77 (2001) 24

[8] Hinchey J, C Chaves, B Appignani, J Breen, L Pao, A Wang, MS Pessin, C Lamy, JL Mas, LR Caplan: A reversible posterior leukoencephalopathy syndrome. N Engl J Med 334 (1996) 494

[9] Jurgensen JS, L Nibbe, KT Hoffmann, L Niehaus: Postpartum blindness. Lancet 358 (2001) 1338

[10] Magpie Trial Collaborative Group: Do Women with preeclampsia, and their babies, benefit from magnesium sulphate? The Magpie Trial: a randomized placebo-controlled trial. Lancet 359 (2002) 1877

[11] Matter F, BM Sibai: Eclampsia. Risk factors for maternal morbidity. Am J Obstet Gynecol 182 (2000) 307

[12] Morris MC, DM Twickler, MR Hatab, GD Clarke, RM Peshok, FG Cunnigham: Cerebral blood flow and cranial magnetic resonance imaging in eclampsia and severe preeclampsia. Obstet Gynecol 89 (1997) 561

[13] National High Blood Pressure Education Program: Working Group Report on High Blood Pressure in Pregnancy. Am J Obstet Gynecol 183 (2000) 51

[14] Peterkin IR, R Wee, RL Desmarais: Reversible cerebral, hepatic and renal lesions in severe preeclampsia. Can Assoc Radiol J 43(1) (1992 Feb) 60

[15] Rutherford JM, A Moody, S Crawshaw, PC Rubin: Magnetic resonance spectroscopy in preeclampsia: evidence of cerebral ischaemia. BJOG 110(4) (2003 Apr) 416

[16] Schaefer PW, FS Buonanno, RG Gonzalez, LH Schwamm: Diffusion-Weighted imaging discriminates between cytotoxic and vasogenic edema in a patient with eclampsia. Stroke 28 (1997) 1082

[17] Schwartz RB, SK Feske, JF Polak, U DeGirolami, A Iaia, KM Beckner, SM Bravo, RA Klufas, RYC Chai, JT Repke: Preeclampsia-Eclampsia: clinical and neuroradiographic correlates and insights into the pathogenesis of hypertensive encephalopathy. Radiology 217 (2000) 371

[18] Weingarten K, D Barbut, C Filippi, RD Zimmerman: Acute hypertensive encephalopathy: Findings on spin-echo and gradient-echo MR imaging. AJR 162 (1994) 664

[19] Williams KP, S Wilson: Persistence of cerebral hemodynamic changes in patients with eclampsia: a report of 3 cases. Am J Obstet Gynecol 181 (1999) 1162

Received October 14, 2004. Revised December 15, 2004. Accepted December 20, 2004.

BJOG: an International Journal of Obstetrics and Gynaecology
July 2004, Vol. 111, pp. 756–757

DOI: 10.1111/j.1471-0528.2004.00179.x

CASE REPORT

Intrauterine therapy for a cytomegalovirus-infected symptomatic fetus

Hideo Matsuda, Yuichi Kawakami, Kenichi Furuya, Yoshihiro Kikuchi

Case report

A 25 year old primigravida presented in July 2001 at 29 weeks of gestation with fetal hydrops. She had flulike symptoms three weeks earlier. On examination, she had no hypertension, proteinuria or any other abnormality. No blood group antibodies were detected. The fetal heart rates showed prolonged non-reassuring patterns on the non-stress test. Over 300 mL of ascites and hepatosplenomegaly were detected on ultrasonography. Maternal serum, amniotic fluid and fetal ascites revealed positive cytomegalovirus (CMV) DNA with quantitative real-time polymerase chain reaction (PCR). Repeated estimation of maternal serum CMV-specific IgM and IgG (enzyme immunoassay [EIA]) did not suggest primary CMV infection. No fetal brain abnormality (swelling, calcification and degeneration) was detected at her presentation with ultrasound and magnetic resonance scans. Percutaneous umbilical blood sampling showed fetal anaemia (haemoglobin: 10.5 g/dL), hypoproteinaemia (total protein: 3.8 g/dL) and elevated liver enzymes (γ-glutamyltranspeptidase: 1458 IU/L). A diagnosis of symptomatic fetal CMV infection was made. Immediate delivery was considered to be contraindicated because of the poor prognosis of neonatal care at this gestational age.[1,2] Conversely, no natural improvement in fetal status was expected because maternal serum CMV-specific IgG were insufficiently high to produce anti-viral immune transfer via placenta (Table 1).

With informed choice, fetal ascites was extracted and CMV high titer gamma globulin, Venoglobulin-IH (polyethyleneglycol treated immunoglobulin; CMV IgG 258.0 of EIA cutoff <2.0, × 199 in the neutraliation test, Benesis, Japan), was injected into the fetal abdominal cavity 2.5 g/fetal body (at most 2 g/estimated fetal weight in kg) using a 23-gauge needle under colour Doppler ultrasound guidance. Every two weeks, three times injection was performed in series. The fetal haemoglobin rose to 12.0 g/dL at 32 weeks and to 12.6 g/dL at 34 weeks of gestation. Fetal growth restriction was observed at presentation but the growth rate returned to normal after the initial treatment. Fetal ascites ceased to be visible at 34 weeks of gestation. Maternal serum CMV-DNA disappeared at 32 weeks of gestation without quantitative alteration of serum IgG and IgM. CMV-DNA in the fetal ascites diminished to undetectable level at 34 weeks of gestation, whereas that in amniotic fluid remained high at 7.6×10^6 to 9.3×10^7 copies/mL until delivery (Table 1).

A 2084 g girl was born by elective section at 36 weeks of gestation following the onset of labour with a flexed breech presentation. Mild villositis with CMV inclusion bodies in the placenta was reported pathologically. CMV-DNA was not detected in the newborn serum and urine. Brain CT scan on day four was reported as normal. Whereas auditory brain reaction on day five predicted slight hearing disturbance in the right side. The newborn was healthy and was hospitalised in our regular newborn care unit for two weeks. At age 24 months, she had a compensating hearing disorder of the right side, but other aspects of her neurological, physical and mental development were normal.

Discussion

Cytomegalovirus is a member of the herpes family of viruses and causes a number of infection syndromes in humans. This includes the classic TORCH syndrome, consisting of hepatosplenomegaly, microcephaly, hyperbilirubinaemia, petechiae, thrombocytopenia, hydrops and intrauterine growth restriction. In symptomatic congenital CMV-infected fetus, mortality may be as high as 20–30%, with 90% of survivors suffering late complication.[1,2] CMV is the most common cause of congenital sensorineural hearing loss.[3] Prenatal diagnosis of CMV-infected fetus remains problematical because of a possible recurrent infection during pregnancy including reactivation of the women's own strain of CMV acquired previously, possible reinfection with a new strain of virus,[4] lack of fetal CMV seropositivity for IgM in culture positive fetuses or failure of the fetus to sustain the IgM response. Ultrasonographic demonstration of significant fetal abnormalities

Department of Obstetrics and Gynaecology, National Defense Medical College, Tokorozawa, Saitama, Japan

Correspondence: Dr H. Matsuda, Department of Obstetrics and Gynaecology, National Defense Medical College, 3-2 Namiki, Tokorozawa, Saitama, 359-1513 Japan.

Table 1. Fetal therapy and quantative analysis of CMV-DNA, IgG and IgM.

	29 weeks 4 days	30 weeks 3 days	31 weeks 4 days	32 weeks 3 days	33 weeks 4 days	34 weeks 3 days	35 weeks 4 days
γ-Globulin injection into fetal abdominal cavity (g)		2.5		2.5		2.5	
Maternal serum CMV-DNA (copy/mL)	180.0	54.0	<20	33.0	<20	<20	<20
Amniotic fluid CMV-DNA (million copies/mL)	7.6		67.0	27.0	80.0	93.0	53.0
Fetal ascites CMV-DNA (thousand copies/mL)	23.0		2.0	0.15	0.12	<0.1	<0.1
Umbilical vein serum CMV-DNA (copy/mL)						<20	
Maternal serum CMV-IgG (EIA cutoff: <2.0)	16.0	15.0	17.0	18.0	23.0	15.0	17.0
Maternal serum CMV-IgM (EIA cutoff: <0.8)	1.84	1.80	1.58	1.72	1.77	1.44	1.55
Umbilical vein serum CMV-IgG (EIA cutoff: <2.0)		2.3		8.4		36.0	

in appropriate clinical circumstances, isolation of the virus or DNA from fluid collected by amniocentesis and haematologic, viral or serological information from fetal blood collected by cordocentesis are all methods for antenatal diagnosis.[5,6] Usually, detected CMV-DNA in amniotic fluid reveals a history of fetal viremia, but it does not directly demonstrate the current fetal condition. An effective fetal therapy remains yet to be found.

Ganciclovir administration into the umbilical vein and anti-CMV IgG injections into the fetal abdominal cavity have been reported but the evaluation of the prognosis is not well established.[7,8] In this case, immunoglobulin was selected over ganciclovir because its administration is safer.[7] Fetal administration was considered preferable to maternal administration because the appropriate dose to reach the fetus via the placenta was difficult to estimate and it would also be expensive. Intravascular administration at the time of percutaneous umbilical blood sampling was also abandoned because its safety for the fetal circulation is not yet proven. Direct intraperitoneal administration was desirable because immunoglobulin would not be diluted by fetoplacental circulation and maternal circulation, and it would minimise the influence of the administered volume of immunoglobulin in the fetal circulation. The dose of immunoglobulin was determined referring to an earlier report.[8]

We conclude that an anti-CMV IgG injection into the fetal abdominal cavity is clinically useful. Our data suggest that, after treatment, CMV-DNA in the amniotic fluid was produced in the infected placenta and the amniotic membrane.

References

1. Stagno S, Whitely RJ. Herpesvirus infections of pregnancy. Part I: Cytomegalovirus and Epstein–Barr virus infections. *N Engl J Med* 1985;**313**:1270–1274.
2. Demmler GJ. Infectious Disease Society of America and Center for Disease Control summary of a workshop on surveillance for congenital cytomegalovirus disease. *Rev Infect Dis* 1991;**13**:315–329.
3. Hicks T, Fowler K, Richardson M, Dahle A, Adams L, Pass R. Congenital cytomegalovirus infection and neonatal auditory screening. *J Pediatr* 1993;**123**:779–782.
4. Boppana SB, Rivera LB, Fowler KB, Mach M, Britt WJ. Intrauterine transmission of cytomegalovirus to infants of women with preconceptional immunity. *N Engl J Med* 2001;**344**:1366–1371.
5. Grose C, Weiner CP. Prenatal diagnosis of congenital cytomegalovirus infection: two decades later. *Am J Obstet Gynecol* 1990;**163**:447–450.
6. Guerra B, Lazzarotto T, Quarta S, et al. Prenatal diagnosis of symptomatic congenital cytomegalovirus infection. *Am J Obstet Gynecol* 2000;**183**(2):476–482.
7. Revello MG, Percivalle E, Baldanti F, et al. Prenatal treatment of congenital human cytomegalovirus infection by fetal intravascular administration of ganciclovir. *Clin Diagn Virol* 1993;**1**:61–67.
8. Negishi H, Yamada H, Hirayama E, et al. Intraperitoneal administration of cytomegalovirus hyperimmunoglobulin to cytomegalovirus-infected fetus. *J Perinatol* 1998;**18**(6):466–469.

Accepted 28 January 2004

J. Perinat. Med. 33 (2005) 561–563 • Copyright © by Walter de Gruyter • Berlin • New York. DOI 10.1515/JPM.2005.100

Short communication

Intrauterine therapy for parvovirus B19 infected symptomatic fetus using B19 IgG-rich high titer gammaglobulin

Hideo Matsuda*, Kenichiro Sakaguchi, Tomoko Shibasaki, Hironori Takahashi, Yuichi Kawakami and Kenichi Furuya

Department of Obstetrics and Gynecology, National Defense Medical College, Japan

Abstract

Parvovirus B19-infected hydrops fetalis was treated using gammaglobulin injection into the peritoneal cavity (GIFPeC) with B19-IgG-rich immunoglobulin. Fetal anemia and hydrops resolved, and B19-DNA in fetal ascites decreased despite no change in maternal B19-IgG or B19-DNA. Gammaglobulin injection into the peritoneal cavity is thus useful for treating hydrops fetalis while avoiding intrauterine blood-transfusion risks.

Keywords: Fetal therapy; gammaglobulin; gammaglobulin injection into fetal peritoneal cavity; parvovirus; pregnancy.

Background

Parvovirus B19-infected hydrops fetalis is known to be fatal in approximately 30% of cases. Conventionally, intrauterine blood transfusion has been used to treat infections occurring around 20 weeks' gestation, the period during which prognosis is regarded as being particularly poor. Although effective, intrauterine blood transfusion poses various problems of technical nature, but also involves risk to the fetus, such as a 6% fetal mortality rate, infection from blood transfusion, and low oxygen transport capacity related to the transfused adult hemoglobin. In the present case, we were able to successfully treat a B19-infected symptomatic fetus with severe anemia without resorting to intrauterine blood transfusion by performing gammaglobulin injection into the peritoneal cavity (GIFPeC).

*Corresponding author:
Hideo Matsuda, MD
Department of Obstetrics and Gynecology
National Defense Medical College
3-2 Namiki
Tokorozawa
Saitama Prefecture
Japan 359-1513
Tel.: 81-42-995-1687
Fax: 81-42-996-5213
E-mail: hmatsuda@ndmc.ac.jp

Case

In May 2004, a 37-year-old woman, gravida 2 para 1, was referred at 20 weeks gestation with fetal hydrops. Three weeks previously she had experienced flu-like symptoms following a diagnosis on her and her 8-year-old daughter of erythema infectiosum. The patient had slight dyspnea and pleural effusion revealed by chest radiology. No blood group antibodies were detected, but fetal ascites, skin edema, pericardial effusion, and cardiomegaly were observed. Cyclic estimation of maternal serum B19-specific IgM and IgG EIA (enzyme immunoassay) suggested a primary B19 infection. Maternal serum, amnion, and fetal ascites tested positive for parvovirus B19-DNA with quantitative real-time polymerase chain reaction (PCR). Ultrasound and magnetic resonance scans did not detect organic fetal anomalies. Doppler ultrasound showed fetal anemia (middle cerebral artery peak systolic velocity (MCAPSV): 0.62 m/s). Based on the patient's symptoms and the above test results, a diagnosis of parvovirus B19-infected hydrops fetalis was made (Table 1).

Methods

With the patient's informed consent, it was decided to perform gammaglobulin injection into the peritoneal cavity (GIFPeC) using B19-IgG-rich immunoglobulin. The National Defense Medical College Hospital, Institutional Review Board approved this treatment.

Fetal ascites fluid was extracted and 0.8 g (approximately 2 g/kg) of parvovirus B19 high titer gammaglobulin (26.2; EIA cut-off: 0.80, Benesis, Japan) injected into the fetal abdominal cavity using a 25-gauge needle (Hanaco Medical, Japan) under color-Doppler-ultrasound guidance. Injections were performed twice, at 21 and 22 weeks duration, at an interval of eight days.

Results

Fetal ascites and pericardial effusion clearly decreased within 5 days and had completely disappeared by

Table 1 Fetal therapy and quantative analysis of B19-DNA, IgG, IgM, and fetal MCA-PSV.

	21w3d	21w4d	22w4d	23w0d	23w3d	28w4d	34w3d	37w2d (delivery)
G-globulin[a] injection into fetal abdominal cavity (g)	0.81		0.81					
Maternal serum B19-DNA (thousand copies/mL)	36.1		34.0		26.0	1.6	0.3	<0.1
Maternal serum B19-IgG (EIA cut off: <0.8)	9.64		9.71		11.67	10.27	8.73	7.10
Maternal serum B19-IgM (EIA cut off: <0.8)	8.87		6.47		5.79	3.52	2.26	1.98
Amniotic fluid B19-DNA (thousand copies/mL)	5700.0				4400.0	45.0	2.70	0.25
Amniotic fluid B19-IgG (EIA cut off: <0.8)	3.94					2.23	1.26	1.29
Fetal ascites B19-DNA (thousand copies/mL)	1000.0		57.0		ascites (-)			
Fetal MCAPSV (m/s)[b]	0.62	0.57	0.40	0.22	0.22	0.35	0.51	
Umbilical vein serum B19-IgG (EIA cut off: <0.8)								7.6
Umbilical vein serum B19-DNA (copy/mL)								<0.1

[a]B19-IgG in g-globulin: 26.7 (EIA cut off: <0.8); [b]MCAPSV: Mean cerebral artery peak systolic velocity

22 weeks gestation, as had maternal dyspnea and pleural effusion. Fetal MCAPSV improved rapidly: 0.57 m/s at 1 day, 0.40 m/s at 7 days, and 0.22 m/s at 11 days after primary injection. Thus, fetal anemia and hydrops improved simultaneously. Furthermore, despite no significant change in either maternal B19-IgG or maternal serum B19-DNA, B19-DNA in the fetal ascites fluid decreased significantly, from 1.0×10^6 copies/mL to 5.7×10^4 copies/mL, by 7 days after treatment.

The patient was released from hospital after two weeks. She was readmitted at 38 weeks gestation for an elective cesarean section and a healthy boy (Apgar score: 8/9) weighing 2,308 g was delivered. No B19-DNA was detected in the newborn's serum, and there was no cardiac dysfunction.

Discussion

Parvovirus B19 is not only cytotoxic for fetal red blood cell precursors (leading to fetal anemia) [1], but also stimulates a cellular process initiating cellular apoptosis (parvovirus myocarditis) [6]. The possibility of B19 infection in pregnancy is estimated to be 3.5% [9] and 8.3–20.0% of infected fetuses die *in utero* [7]. Risk is highest in the first trimester, with 10.0–23.1% spontaneous abortions or fetal deaths prior to 20 weeks gestation [7, 9]. Hydrops fetalis resulting from fetal anemia can lead extremely rapidly to death [4], but resolves spontaneously in 34% of cases [3, 8].

Doppler assessment of fetal MCAPSV is an accurate tool for determining fetal anemia and is a non-invasive alternative to cordocentesis [2] and was used to gauge treatment efficacy in the present study because of the possible risks of cordocentesis. However, fetal treatment without cordocentesis is not yet established. One case of a parvovirus B19-infected woman being treated intravenously with gammaglobulin during pregnancy has been documented [10], but this method is not cost-effective. Rodis et al. [8] have shown intrauterine transfusion to be an effective treatment, reporting recovery in 29% of cases after intrauterine transfusion versus death in 30% without intervention. However, they also reported death after transfusion in as many as 6% of case. Since this report does not record parvovirus B19 antibody levels in the transfused blood, it is unclear whether the recoveries were due to the transfusion of adult blood or to B19 antibodies in the transfused blood.

Gammaglobulin injection into the peritoneal cavity (GIFPeC) has already been used to treat a cytomegalovirus-infected symptomatic fetus [5], and is a comparatively safe treatment method in that it avoids cordocentesis. Peritoneal injection avoids direct preload on fetal circulation during the procedure and enables administration of higher quantities. As gammaglobulin is a heated blood product, the risk of infection is lower than that of blood transfusion. Furthermore, since package inserts list viral antibody levels, it is possible to order and use vials containing high levels of antibodies to specific viruses. Such factors, combined with the results obtained in this case, indicate that gammaglobulin injection into the peritoneal cavity (GIFPeC) may be a clinically useful therapy for parvovirus B19-infected hydrops fetalis.

References

[1] Brown KE, SM Anderson, NS Young: Erythrocyte P antigen: Cellular receptor for B19. Science 262 (1993) 114

[2] Cosmi E, G Mari, LD Chiaie, et al.: Noninvasive diagnosis by Doppler ultrasonography of fetal anemia resulting from parvovirus infection. Am J Obstet Gynecol 187 (2002) 1290
[3] Fairley C, J Smoleniec, O Caul, E Miller: Observational study of effect of intrauterine transfusions on outcome of fetal hydrops after parvovirus B19 infection. Lancet 346 (1995) 1335
[4] Jordan J: Identification of human parvovirus B19 infection in idiopathic nonimmune hydrops fetalis. Am J Obstet Gynecol 16 (1996) 342
[5] Matsuda H, Y Kawakami, K Furuya, Y Kikuchi: Intrauterine therapy for cytomegalovirus infected symptomatic fetus. BJOG 111 (2004) 756
[6] More AL, DJ Ferguson, KA Flemming: Ultrastructural features of fetal erythroid precursors infected with parvovirus B-19 *in-vitro*: Evidence of cell death by apoptosis. J Pathol 169 (1993) 213
[7] Public Health Laboratory Service Working Party on Fifth Disease. Prospective study of human parvovirus (B19) infection in pregnancy. BMJ 300 (1990) 1166
[8] Rodis JF, AF Borgida, M Wilson, et al.: Management of parvovirus infection in pregnancy and outcomes of hydrops: A survey of members of the Society of Perinatal Obstetricians. Am J Obstet Gynecol 179 (1998) 985
[9] Rodis JF, DL Quinn, WJ Garry, et al.: Management and outcomes of pregnancies complicated by Human B19 parvovirus infection: A prospective study. Am J Obstet Gynecol 163 (1990) 1168
[10] Selbing A, A Josefuson, LO Dahle, R Lindgren: Parvovirus B19 infection during pregnancy treated with high-dose intravenous gammaglobulin. Lancet 345 (1995) 660

Received July 7, 2005. Accepted July 22, 2005.

JOURNAL OF VIROLOGY, Oct. 2005, p. 12871–12879
0022-538X/05/$08.00+0 doi:10.1128/JVI.79.20.12871–12879.2005

Vol. 79, No. 20

Priming-Boosting Vaccination with Recombinant *Mycobacterium bovis* Bacillus Calmette-Guérin and a Nonreplicating Vaccinia Virus Recombinant Leads to Long-Lasting and Effective Immunity

Yasushi Ami,[1] Yasuyuki Izumi,[2] Kazuhiro Matsuo,[2] Kenji Someya,[2] Masaru Kanekiyo,[2] Shigeo Horibata,[2] Naoto Yoshino,[4] Koji Sakai,[2] Katsuaki Shinohara,[3] Sohkichi Matsumoto,[5] Takeshi Yamada,[6] Shudo Yamazaki,[2] Naoki Yamamoto,[2] and Mitsuo Honda[2]*

Division of Experimental Animal Research,[1] AIDS Research Center,[2] and Division of Biosafety Control and Research,[3] National Institute of Infectious Diseases, Toyama 1-23-1, Shinjuku-ku, Tokyo 162-8640, Japan; Department of Microbiology and Immunology, Iwate Medical University School of Medicine, Uchimaru 19-1, Morioka, Iwate 020-8505, Japan[4]; Department of Host Defense, Graduate School of Medicine, Osaka City University, Osaka, Osaka 545-8585, Japan[5]; and Department of Bacteriology, School of Dentistry, Nagasaki University, Nagasaki, Nagasaki 852-8588, Japan[6]

Received 29 April 2005/Accepted 22 July 2005

Virus-specific T-cell responses can limit immunodeficiency virus type 1 (HIV-1) transmission and prevent disease progression and so could serve as the basis for an affordable, safe, and effective vaccine in humans. To assess their potential for a vaccine, we used *Mycobacterium bovis* bacillus Calmette-Guérin (BCG)-Tokyo and a replication-deficient vaccinia virus strain (DIs) as vectors to express full-length *gag* from simian immunodeficiency viruses (SIVs) (rBCG-SIVgag and rDIsSIVgag). Cynomolgus macaques were vaccinated with either rBCG-SIVgag dermally as a single modality or in combination with rDIsSIVgag intravenously. When cynomologus macaques were primed with rBCG-SIVgag and then boosted with rDIsSIVgag, high levels of gamma interferon (IFN-γ) spot-forming cells specific for SIV Gag were induced. This combination regimen elicited effective protective immunity against mucosal challenge with pathogenic simian-human immunodeficiency virus for the 1 year the macaques were under observation. Antigen-specific intracellular IFN-γ activity was similarly induced in each of the macaques with the priming-boosting regimen. Other groups receiving the opposite combination or the single-modality vaccines were not effectively protected. These results suggest that a recombinant *M. bovis* BCG-based vector may have potential as an HIV/AIDS vaccine when administered in combination with a replication-deficient vaccinia virus DIs vector in a priming-boosting strategy.

As the rate of new infections with human immunodeficiency virus type 1 (HIV-1) continues to increase globally, an effective preventive vaccine is urgently needed to stem further spread of the virus (24). Because long-term survival in humans has been observed when HIV-1 replication is controlled by protective immunity (12, 29), targeted experimental immunogens have been designed to closely mimic the long-lasting protective immunity induced in long-term human survivors by the natural infection (8, 25). Recently, various vaccine modalities, including live viral vectors and DNA, have been used to elicit protective immunity in nonhuman primate models (9). However, before an HIV-1 vaccine regimen can be considered promising, it must be shown to be not only effective at inducing protective immunity, but also safe, affordable, and compatible with other vaccines (2, 32).

When it comes to safety, traditional live vaccines, which have been administered safely to both the healthy and the infected, may be the vectors of choice for HIV-1 vaccines. In order to fully take advantage of the potential benefits of traditional live vectors in HIV-1 vaccine development, we studied the *Mycobacterium bovis* bacillus Calmette-Guérin (BCG) substrain Tokyo 172 (6) and the replication-deficient vaccinia virus vaccine strain DIs (22, 50), both of which have been shown to be nonpathogenic when inoculated into immunodeficient animals (41, 51, 53) as live recombinant vaccine vehicles (1, 17–19, 46–48). As further evidence of the potential of the live vectors for use in HIV/AIDS vaccines, we noted that a recombinant *M. bovis* BCG vector candidate vaccine for HIV-1-induced positive immune responses in animals (17, 46). Moreover, we found that recombinant vaccinia virus DIs encoding the simian immunodeficiency virus (SIV) gene was effective at eliciting anti-SIV immunity in mice when administered as a booster antigen after priming with SIV DNA (47). In this study, we have developed a new combination regimen, priming with recombinant *M. bovis* BCG-SIV Gag followed by boosting with rDIsSIVgag. This immunization regimen elicited effective positive immunity against an immune deficiency virus in macaques for the 1 year they were under study.

MATERIALS AND METHODS

Animals and virus challenge stocks. All animals used in this study were captive bred and obtained from the Philippines. They were mature, cycling, male cynomologus macaques (*Macaca fascicularis*) from the Tsukuba Primate Center, the National Institute of Infectious Diseases, Japan. Animals used in these studies were free of known simian retroviruses, herpes viruses, bacteria, and parasites. They were housed in accordance with the Guidelines for Animal Experimenta-

* Corresponding author. Mailing address: AIDS Research Center, National Institute of Infectious Diseases, Toyama 1-23-1, Shinjuku-ku, Tokyo 162-8640, Japan. Phone: 81-3-5285-1111, ext. 2737. Fax: 81-3-5285-1183. E-mail: mhonda@nih.go.jp.

tion of the Japanese Association for Laboratory Animal Science, 1987, under the Japanese Law Concerning the Protection and Management of Animals (46) and were maintained in accordance with the guidelines set forth by the Institutional Animal Care and Use Committee of National Institute of Infectious Diseases, Japan. Once approved by an institutional committee for biosafety level 3 experiments, these studies were conducted at the Tsukuba Primate Center, National Institute of Infectious Diseases, Japan, in accordance with the requirements specifically stated in the laboratory biosafety manual of the World Health Organization. The animals' condition was monitored by analyzing a hemogram parameter as well as absolute $CD4^+$ and $CD8^+$ T-lymphocyte counts with an automated blood analyzer Celltac (Nihon Koden, Tokyo Japan), as described below.

Two thousand 50% tissue culture infectious doses ($TCID_{50}$) of SHIV KS661c, a pathogenic molecular clone, were intrarectally administered as a challenge virus (39). The parent virus, SHIV-C2/1, is an SHIV-89.6 variant isolated by in vivo passage in cynomolgus macaques (40, 42) and the original SHIV-89.6 strain was kindly provided by Y. Lu at the Harvard AIDS Institute (Boston, MA) (26, 37). SHIV-C2/1 and SHIV KS661c were shown to infect cynomologus macaques by both the intravenous and intrarectal routes (39). Both viruses induced high levels of viremia and marked $CD4^+$ T-cell depletion within 2 and 3 weeks after inoculation, respectively (39, 40, 42). Virus stocks were stored at −125°C and thawed just prior to use.

Production and preparation of recombinant *M. bovis* BCG (rBCG) and vaccinia virus DIs expressing full-length SIV Gag. Detailed methods for plasmid construction were described previously (7, 17, 18, 21). Briefly, a DNA fragment encoding the full-length *gag* sequence of SIVmac239 was cloned downstream of the *hsp60* promoter (52) and then inserted into the multicloning site of the plasmid pSO246 (28). Recombinant *Mycobacterium bovis* BCG substrain Tokyo 172 that stably expressed the inserted DNA fragment (designated rBCG-SIVgag) was then selected and used for all rBCG inoculations. For the Western blot analysis, the transformant of rBCG was grown in 7H9-ADC broth for 2 weeks and a portion of the culture medium was periodically collected, sonicated and blotted using the monoclonal antibody IB6, as described previously (47). Since the recombinant DIs virus (rDIs) encoding the SIVmac239 *gag-pol* open reading frame elicited remarkably high SIV Gag-specific T-cell responses but low polymerase responses in mice (47), confirming the findings of a previous report (20), we named it rDIsSIVgag. The rDIsSIVgag and rDIs encoding β-galactosidase (rDIsLacZ) were prepared with chicken embryo fibroblast (CEF) cells (18, 47). Virus preparations were purified by sucrose density gradient ultracentrifugation and were adjusted to 10^7 PFU/ml. P27 antigen generation in cells was measured by antigen-specific enzyme-linked immunosorbent assay (42).

Virus-specific IFN-γ ELISPOT assays. ELISPOT assays were performed using the method developed by and following the direct instructions of Mothe and Watkins, Wisconsin University Primate Center (31, 46). In brief, 96-well flat-bottomed plates (U-CyTech-BV, Utrecht, Netherlands) were coated with anti-gamma interferon (IFN-γ) monoclonal antibody MD-1 (U-CyTech-BV). Freshly isolated peripheral blood mononuclear cells (PBMC) were added with either concanavalin A or pooled Gag peptides (AIDS Research and Reference Reagent Program, National Institutes of Health, Rockville, MD). The cells were then incubated in anti-IFN-γ-coated plates before lysing with ice-cold deionized water. After plates had been washed, rabbit anti-IFN-γ polyclonal biotinylated detector antibody (1 μg per well; U-CyTech-BV) was added. The plates were reacted with gold-labeled antibiotin immunoglobulin G solution by adding 30 μl of the activator mix (U-CyTech-BV) to each of the wells and allowing them to develop for 15 min.

Wells were imaged and spot-forming cells (SFC) were counted using the KS ELISPOT compact system (Carl Zeiss, Germany) (31, 46). An SFC was defined as a large black spot with a fuzzy border. To determine significance levels, we established a baseline for each peptide using the average and standard deviation of the number of SFC for each peptide. A threshold significance value corresponding to this average and two standard deviations were then determined. A response was considered positive if the number of SFC exceeded the threshold significance level of the sample with no added peptide.

Detection of intracellular IFN-γ by flow cytometry. Intracellular macaque IFN-γ was detected by intracellular IFN-γ cytokine staining as previously described (30). Briefly, freshly isolated PBMC was incubated with antigen for 16 h at 37°C with 5% CO_2. During the final 6 to 8 h, brefeldin A (Sigma Chemical Co., St. Louis, MO) was added at 10 μg/ml. Antibody to CD28 (1 μg/ml, BD Pharmingen, San Diego, CA) was also added during the incubation as a costimulator molecule. After stimulation, the cells were stained with fluorescein isothiocyanate-conjugated anti-CD3 (FN18; Biosource, Camarillo, CA) and peridinin chlorophyll protein-conjugated anti-CD8 antibodies (Leu-2a; Becton Dickinson Biosciences, San Jose, CA). The cells were then sequentially incubated with fluorescence-activated cell sorter (FACS) lysing solution (Becton Dickinson) for 10 min and FACS permeabilizing solution (Becton Dickinson) for another 10 min. The cells were washed, stained with phycoerythrin-conjugated anti-human IFN-γ antibody (4S.B3; BD Pharmingen), and fixed with 2% paraformaldehyde. Samples were analyzed with a FACSCalibur using Cell Quest software (Becton Dickinson).

Lymphocyte proliferative responses. SIV-specific proliferative responses were measured in freshly isolated PBMC as described by Gauduin et al. and Hel et al. (14, 15). PBMC were cultured in flat-bottomed 96-well plates with either concanavalin A or purified SIVmac251 p27 protein (Advanced BioScience Laboratories, Rockville, MD) (15) for three days before the addition of [^{3}H]thymidine. Cells were harvested 16 h later to determine uptake.

Absolute $CD4^+$ and $CD8^+$ T-lymphocyte counts. An absolute cell count of peripheral blood was measured as previously described (55). Briefly, 50 μl of whole blood was placed in a polypropylene tube and incubated with FITC-conjugated monoclonal anti-CD3 (FN18; Biosource), phycoerythrin-conjugated anti-CD4 (Leu-3a; Becton Dickinson), and peridinin chlorophyll protein-conjugated anti-CD8 (Leu-2a; Becton Dickinson) antibodies at 4°C. After incubation with FACS lysing solution (Becton Dickinson), the cells were analyzed with a FACSCalibur using Cell Quest software (Becton Dickinson).

Plasma viral RNA copy numbers. Plasma viral RNA copy numbers were measured using a real-time quantification assay based on the TaqMan system (Applied Biosystems, Foster City, CA) and the Prism 7700 sequence detection system (Applied Biosystems), as reported previously (30, 46). Briefly, viral RNA was extracted and purified from macaque plasma samples using a QIAamp viral RNA mini kit (QIAGEN, Valencia, CA). The RNA was subjected to reverse-transcription and amplification using a TaqMan EZ RT-PCR Kit (Applied Biosystems) with SIV Gag consensus primers SIVmac239-1224F and SIVmac239-1326R, and the SIV Gag consensus Taqman probe FAM-SIV-1272T. To obtain control RNA for quantification, SIVmac239 *gag* RNA was synthesized using T7 RNA polymerase and pKS460, a template plasmid that contains SIVmac239 *gag* under control of the T7 promoter.

To measure the RNA recovery rate, 10^5 copies of SHIV KS661c, in which the viral RNA copy number was previously determined by branched DNA assay (Bayer), were extracted and purified using the same kit as for the sample. Plasma viral load was calculated based on the standard curve of control RNA and the RNA recovery rate. All assays were carried out in duplicate.

Statistical analysis. Data analysis was carried out using the Stat View program (SAS Institute, Cary, NC) and data are expressed as the mean ± standard deviation. A P value of <0.05 was considered significant.

RESULTS

Construction and preparation of recombinant *M. bovis* BCG Tokyo 172 and vaccinia virus DIs expressing whole SIV Gag. In initial studies, we cloned DNA encoding SIVmac239 *gag* downstream of the *hsp60* promoter and the expression unit was inserted into the KpnI restriction site of plasmid pSO246. We also constructed a recombinant *M. bovis* BCG vaccine based on the Tokyo 172 strain expressing the full-length *gag* gene of SIVmac239 (rBCG-SIVgag) (Fig. 1A). The presence of SIV Gag-specific DNA was confirmed in recombinant bacteria by DNA-PCR (42). To determine the in vitro expression of the SIV Gag protein in the cells, we analyzed cell extracts of rBCG-SIVgag bacteria after 2 weeks of culture by Western blot using anti-SIV Gag monoclonal antibody IB6. The rBCG clone produced an SIV Gag recombinant protein that strongly reacted as a single band with the specific monoclonal antibody (Fig. 1B). The concentration of SIV Gag^{p27} protein in transformed bacteria was 28.56 ± 8.30 ng/10^8 CFU of bacilli. In contrast, neither SIV Gag protein nor *gag* DNA was detected in bacteria transformed with rBCG-pSO246, a control construct lacking the SIV *gag* insert and used as a vector control (Fig. 1B).

rDIsSIV*gag* and a control vaccinia virus, rDIsLacZ, were propagated in CEF and adjusted to 10^7 PFU/ml. Using Western blot, we confirmed the expression of each foreign gene in

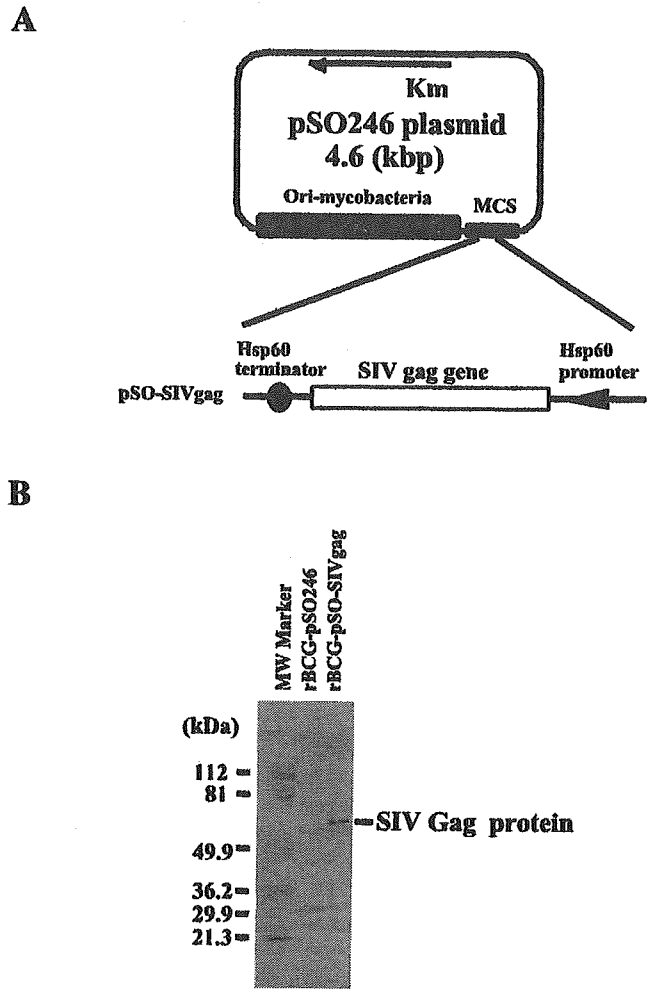

FIG. 1. Vector construction and expression of rBCG-SIVgag. (A) Construction of the expression vector pSO-SIVgag. Full-length DNA of SIVmac239 *gag* was inserted into the multicloning site of pSO246 and expressed in the vaccine strain *M. bovis* BCG Tokyo 172. (B) Detection of SIV Gag protein by Western blot with anti-p27 Gag monoclonal antibody IB6.

the cell extract, and purified virions used as immunogens in this study.

Immune induction after single-modality or combined immunization regimens with vaccine candidates. We examined whether rBCG expressing the full-length *gag* gene of SIVmac239 would be suitable for use in combined prime-boost protocols with the replication-deficient vaccinia virus strain DIs recombinant. The rBCG was intradermally delivered to the inner region of the thigh and rDIs was intravenously administered into the small saphenous vein on the back of the leg. Of the 15 macaques registered in this study, 13 were divided into five groups and immunized using either a single-modality regimen plus vector controls or with a priming-boosting regimen consisting of *M. bovis* BCG and vaccinia virus DIs recombinants (Table 1). The remaining two macaques were inoculated with phosphate-buffered saline and served as naïve controls throughout the experiment.

Group 1 (control group, $n = 3$) served as a vector control group that received rBCG-pSO246 intradermally followed by two inoculations of rDIsLacZ intravenously; group 2 (rBCG group, $n = 2$) received rBCG-SIVgag intradermally followed by two inoculations of rDIsLacZ intravenous, while group 3 (rBCG/rDIs group, $n = 3$) received rBCG-SIVgag intradermally followed by two inoculations of rDIsSIVgag intravenously. Finally, group 4 (rDIs group, $n = 2$) received two inoculations of rDIsSIVgag intravenously followed by rBCG-pSO246 intradermally, while group 5 (rDIs/rBCG group, $n = 3$) received two inoculations of rDIsSIVgag intravenously followed by rBCG-SIVgag intradermally. The 13 immunized and two naive animals were studied for immune induction for 64 weeks before being mucosally challenged with virulent SHIV for a period of 1 year (Table 1).

Antigen-specific T-cell responses in all 15 animals were monitored by SIV Gag peptide-specific IFN-γ-ELISPOT assays (Fig. 2). Fifty weeks postinfection, the rBCG/rDIs group showed the highest SIV Gag-specific IFN-γ-ELISPOT responses; that group's responses peaked at 1,020 ± 360 SFC/10^6 PBMC at 56 weeks postinfection or 2 weeks after the second booster inoculation (Fig. 2A). At 56 weeks postinfection, the ELISPOT responses of the rDIs/rBCG group (380 ± 35 spots per million PBMC, Fig. 2B) were significantly lower than those of the rBCG/rDIs group ($P < 0.05$), as were the ELISPOT

TABLE 1. Immunization and challenge schedule[a]

Group no. (regimen)	Macaque no.	Priming immunization, route, and schedule	Boost immunization, route, and schedule	Mucosal challenge[b]
1 (control)	06, 90, and 91	rBCG-pSO246, 10 mg, i.d., wk 0	rDIsLacZ, 10^6 PFU, i.v., wk 47 and 54	2,000 $TCID_{50}$, i.r., wk 64
2 (rBCG)	29 and 93	rBCG-SIV *gag*, 10 mg, i.d., wk 0	rDIsLacZ, 10^6 PFU, i.v., wk 47 and 54	2,000 $TCID_{50}$, i.r., wk 64
3 (rBCG/rDIs)	08, 10, and 46	rBCG-SIVgag, 10 mg, i.d., wk 0	rDIsSIVgag, 10^6 PFU, i.v., wk 47 and 54	2,000 $TCID_{50}$, i.r., wk 64
4 (rDIs)	01 and 42	rDIsSIVgag, 10^6 PFU, i.v., wk 0 and 8	rBCG-pSO246, 10 mg, i.d., wk 54	2,000 $TCID_{50}$, i.r., wk 64
5 (rDIs/rBCG)	85, 36, and 40	rDIsSIVgag, 10^6 PFU, i.v., wk 0 and 8	rBCG-SIVgag, 10 mg, i.d., wk 54	2,000 $TCID_{50}$, i.r., wk 64

[a] Vaccines, immunization, and challenge studies for all the macaques are described in the text. Animal studies were simultaneously conducted using cynomolgus macaques. i.d., intradermal inoculation; i.v., intravenous inoculation; i.r., intrarectal inoculation.

[b] All of the animals were mucosally challenged with virulent SHIV KS661c at 64 weeks postimmunization and were observed for at least 1 year or, if they did not survive for a year, until the time of their death.

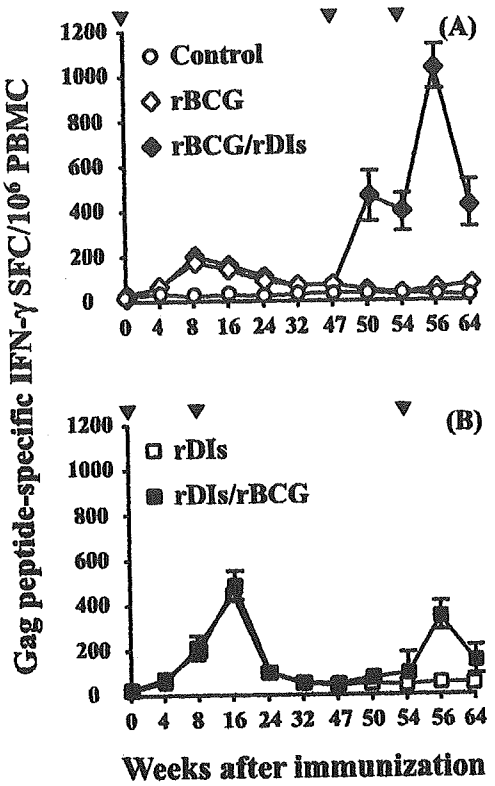

FIG. 2. Kinetics of SIV Gag peptide-specific IFN-γ spot-forming cell responses. PBMC freshly isolated from macaques immunized with either rBCG-SIVgag or rDIsSIVgag alone or with the two in combination were assessed for their ability to produce IFN-γ in response to stimulation by overlapping peptides that span the SIV Gag protein. Arrows indicate inoculation dates of the rBCG/rDIs, rBCG,and control groups, and error bars represent mean ± standard deviation.

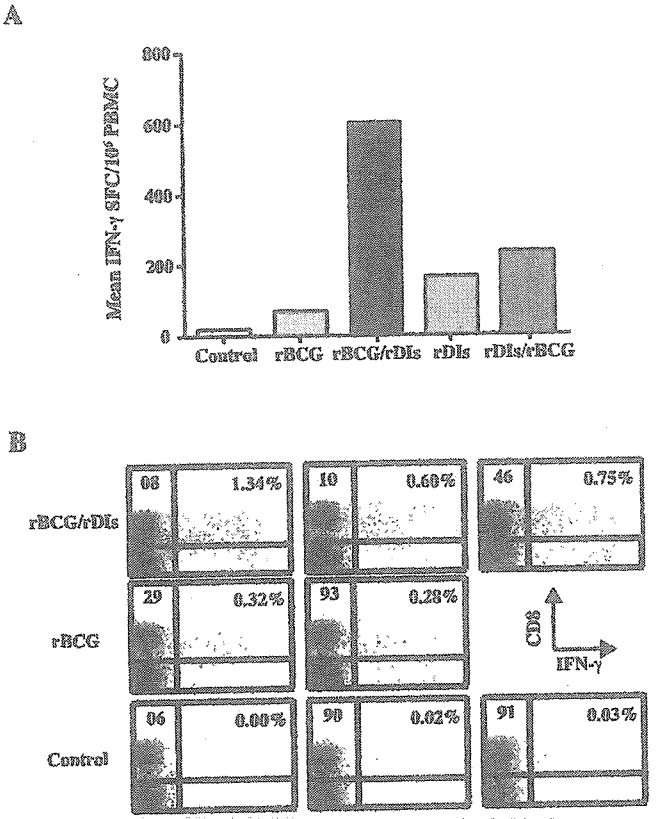

FIG. 3. SIV Gag-specific IFN-γ production in both $CD8^+$ and non-$CD8^-$ T cells in animals immunized with the rBCG/rDIs priming-boosting regimen. (A) SIV Gag protein-specific IFN-γ Elispot responses in immunized monkeys. Monkey PBMC were prepared 2 weeks after final boosting, and 2×10^5 cells were stimulated with 2 μg of recombinant SIV Gag p27 antigen protein. The bars indicate mean values of antigen-specific IFN-γ spot-forming cells per 10^6 PBMC. (B) Flow cytometric analysis of IFN-γ-producing T cells specific for SIV Gag. PBMC from macaques were cultured in vitro with overlapping peptides and stained for intracellular IFN-γ. The percentage of IFN-γ-producing $CD8^+$ T cells in each macaque's PBMC was determined by flow cytometry 2 weeks after final boosting.

responses in other rBCG and rDIs groups, both at 56 weeks postinfection and before mucosal challenge with pathogenic SHIV ($P < 0.05$). Furthermore, the number of SFC in the control and in the two naïve macaque groups did not exceed twenty during the 64-wk immunization period. Thus, the two booster inoculations of rDIs in rBCG-immunized animals effectively induced Gag peptide-specific IFN-γ-ELISPOT responses in peripheral blood, with the booster effect of DIs somewhat resembling that observed in our previous report on DNA/DIs prime-boost immunization in mice (47).

We further studied the induction of SIV Gag-specific IFN-γ ELISPOT by stimulating PBMC with SIV Gag^{p27} protein 56 weeks postinfection (Fig. 3A). The rBCG/rDIs group expressed whole-protein-specific IFN-γ responses of 615 ± 49 cells per million PBMC and the highest peptide-specific ELISPOT responses at 56 weeks postinfection (Fig. 2) of all five groups, with the peptide-specific responses being higher than the protein-specific responses (Fig. 2 and 3A). Other groups exhibited fewer than 200 cells per million PBMC.

To characterize the cellular immune responses in the rBCG/rDIs group, PBMC from the rBCG/rDIs-immunized macaques were compared with those of the rBCG and control groups by staining the surface for CD8 and intracellular SIV Gag-specific IFN-γ expression ($CD8^+$IFN-γ^+ cells) and then performing flow cytometric analysis (Fig. 3B). In vitro stimulation of PBMC with SIV Gag peptides in macaques 08, 10, and 46 of the rBCG/rDIs group generated a higher percentage of $CD8^+$ IFN-γ^+ T cells (1.34, 0.60, and 0.75%, respectively) than it did in animals of the rBCG group. Furthermore, non-$CD8^+$ T cells in PBMC from each animal of the rBCG/rDIs group expressed higher levels of SIV Gag-specific IFN-γ activities (macaque 8: 0.42%; macaque 10: 0.29%; macaque 46: 0.55%) than did those of the other two animal groups. The vector control animals had fewer than 0.03% of both $CD8^+$ IFN-γ^+ and non-$CD8^+$ IFN-γ^+ double-positive cells in PBMC. These findings show that the rBCG/rDIs prime-boost immunization augmented numbers of both IFN-γ-specific intracellular staining-positive cells and ELISPOT in the immunized animals, and that antigen-specific IFN-γ activities were highly induced in $CD8^+$ as well as in non-$CD8^+$ T cells, the latter most likely being $CD4^+$ T cells.

Mucosal challenge study with virulent SHIV KS661c for vaccine efficacy. Ten weeks after the second booster immunization or 64 weeks postinfection, the macaques were chal-

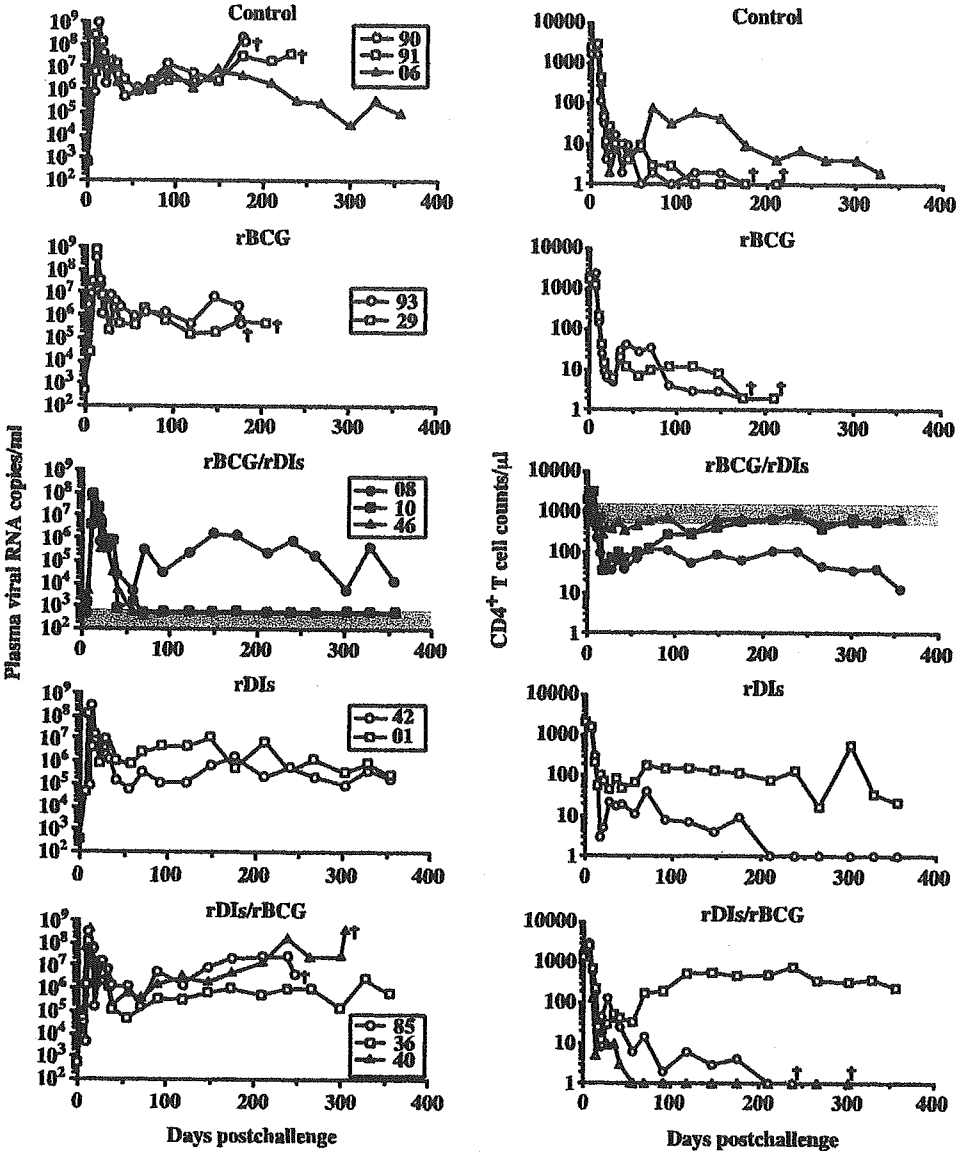

FIG. 4. Plasma viral loads and CD4 T-cell counts after viral challenge. Postchallenge plasma viral RNA copies and absolute CD4 T-cell counts in peripheral blood were detected in macaques in each of five groups immunized with a consecutive prime-boost regimen consisting of rBCG-SIVgag and rDIsSIVgag. In the study, 13 macaques were divided into five groups following the experimental designs described in Table 1.

lenged by intrarectal inoculation with 2×10^3 $TCID_{50}$ or 50 50% monkey infectious doses (MID_{50}) of SHIV KS661c, a molecular clone derived from an SHIV-89.6 variant. As shown in Fig. 4, only those macaques in the rBCG/rDIs group first primed with rBCG-SIVgag and then boosted with two inoculations of rDIsSIVgag showed evidence of protective immune responses (rBCG/rDIs). For two animals in this group (macaques 10 and 46), plasma viremia levels remained undetectable (<500 RNA copies/ml, shadow in left panel of rBCG/rDIs in Fig. 4) and $CD4^+$ T-cell counts stayed above 500 cells/μl (shadow in right panel of rBCG/rDIs in Fig. 4) for the entire year of testing. The third animal in this group (macaque 08) had fluctuating levels of viremia that were still significantly lower than those of animals in the other immunization groups. Coincidentally, this animal also had significantly decreased $CD4^+$ T-cell counts.

All macaques in the rBCG/rDIs group remained clinically healthy during the one-year observation period. Those in the rDIs/rBCG group maintained antigen-specific immune responses (Fig. 6), but showed no protective immunity against viral challenge, except for macaque 36 who showed fluctuation in the number of $CD4^+$ T cells, with numbers dipping at times below 500 cells/μl (rDIs/rBCG in Fig. 4). macaques in the other three groups all showed high levels of plasma viremia and a loss of $CD4^+$ T cells, suggesting that vaccination with rBCG and rDIs, either alone or as a priming agent, may not be suitable to induce effective, long-term positive immunity against mucosal challenge by virulent virus. By day 170 after

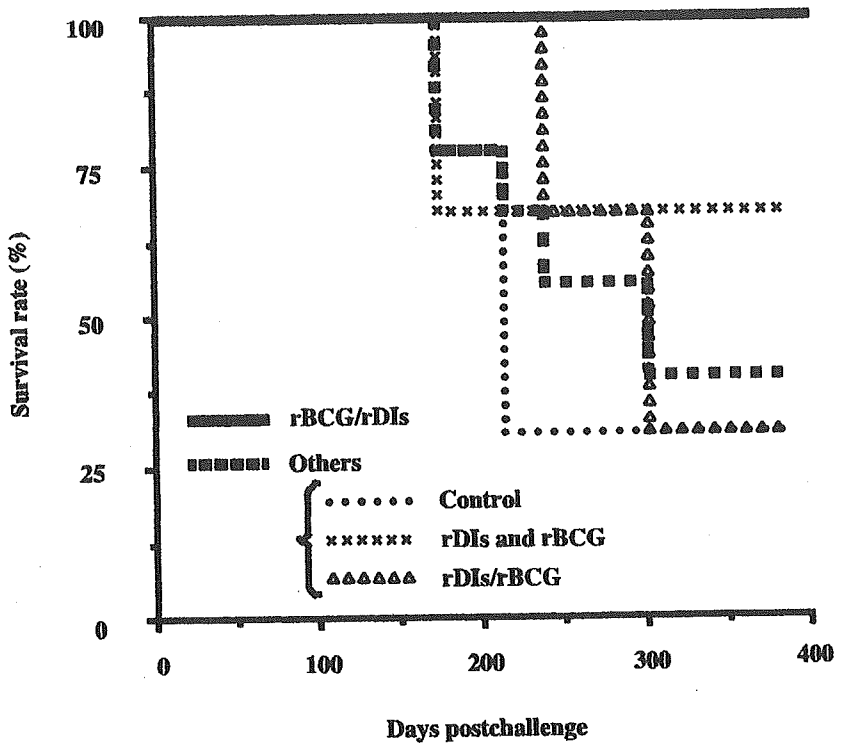

FIG. 5. Survival rates of immunized and control macaques in each of the five immunization groups. A Kaplan-Meier plot of cumulative survival rates at 1 year postchallenge with pathogenic SHIV is shown. The bold line represents group 3 immunized with the rBCG/rDIs priming-boosting regimen; the rectangular broken line represents the mean value for the total number of animals in groups 1, 2, 4, and 5.

challenge, six of the 13 macaques had died with symptoms consistent with simian AIDS: four with interstitial pneumonia, one with neurological disturbances, and one with acquired hemorrhagic diathesis. Analysis of the cumulative survival rate using the Kaplan-Meier plot showed that the rBCG/rDIs group vaccinated with the priming-boosting regimen had a superior survival rate ($P = 0.012$) to the other groups receiving vaccine protocols ($P = 0.548$) and to the control group (Fig. 5). These findings demonstrate that a prime-boost immunization with rBCG-SIVgag/rDIsSIVgag controlled virulent immunodeficiency virus infection in macaques for at least 1 year and more significantly improved survival rates than did other vaccine protocols.

Immune correlates of protection after viral challenge. In order to study virus-specific immune enhancement by SHIV challenge, we followed the postchallenge expansion of the virus-specific IFN-γ-positive cells in each animal by comparing the virus-specific IFN-γ-positive cell numbers pre- and postchallenge (Fig. 6). In all of the challenged animals of the rBCG/rDIs group, the mean number of IFN-γ-positive cells expanded from 369 ± 73 at the time of viral challenge to 629 ± 41 cells per 10^6 PBMC at 7 days after viral challenge, the sharpest increase noted with any of the animal groups. The animals of the rDIs/rBCG group showed much less enhancement, from a mean of 108 ± 46 cells per 10^6 PBMC before challenge to 224 ± 64 postchallenge, demonstrating that cellular immune responses are enhanced by viral challenge in the initial viral infection period in animals. Although in the rBCG/rDIs group high levels of IFN-γ production were observed in both $CD8^+$ and non-$CD8^+$ T cells in all three monkeys, macaque 10 and macaque 46 maintained undetectable setpoint levels of plasma viral load and normal numbers of $CD4^+$ lymphocytes, while macaque 08 did not. The macaques showed no clinical sign of weight loss, lymphoadenopathy, splenomegaly, anemia, or thrombocytopenia in the 1-year observation period. Furthermore, macaques in the rDIs group survived under low

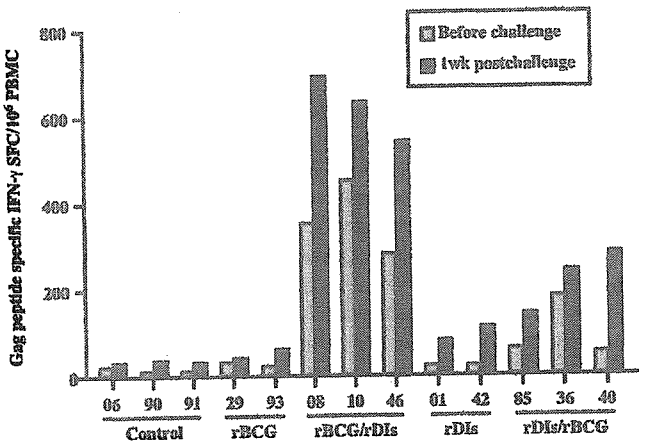

FIG. 6. Virus challenge enhances the SIV Gag peptide-specific IFN-γ ELISPOTs in PBMC from immunized macaques. PBMC from immunized animals were tested with pools of peptides spanning all the proteins from SIVmac239. Results show the production of IFN-γ to pooled peptides in $CD8^+$ and non-$CD8^-$ T lymphocytes.

immune induction but exhibited $CD4^+$ T-cell loss and plasma viremia. Notably, all macaques in the control group exhibited very low levels of immune induction by viral challenge and showed no viral control.

DISCUSSION

In the current study, we initially produced rBCG expressing SIV whole Gag. Second, by introducing a priming-boosting regimen combining rBCG-SIVgag with a nonreplicating rDIsSIVgag, we found that the rBCG/rDIs vaccination induced a long-lasting and effective immunity that was able to control a highly pathogenic virus after mucosal challenge in macaques. Third, elicitation of virus-specific immunity was observed to be important in exerting viral control in the animals immunized with the prime-boost vaccine regimen. Further investigation using larger groups of animals will be needed to determine whether high levels of immune induction correlate with increased efficacy. In this study, the macaques in the rBCG/rDIs group developed high levels of cellular immunity and were protected against the loss of $CD4^+$ T lymphocytes and the increase of viral RNA levels induced by viral challenge. Furthermore, the rBCG/rDIs group showed no evidence of clinical diseases or mortality after viral challenge during the 1-year period of observation.

The rBCG/rDIs prime-boost vaccine controlled the infection efficiently for the duration of the one-year observation period, reducing viral loads to below the threshold level for RNA copies in peripheral blood and maintaining the $CD4^+$ cell numbers above 500 cells per microliter of peripheral blood in two of the three animals in group 3. The remaining animal in the group showed fluctuations in the two parameters. Viral loads and $CD4^+$ cell numbers were not significantly affected in animal groups following the other vaccine regimens. The level of vaccine efficacy for the rBCG/rDIs group seems to be comparable to that observed in previous studies with DNA/fusion protein of interleukin-2 and immunoglobulin G (5), DNA/MVA (3), DNA/recombinant adenovirus type 5 (Ad5) (45), and MVA/recombinant vesicular stomatitis virus (36); that is, effective control of pathogenic SHIV 89.6P infection was achieved in macaques for 6 to 8 months.

SHIV KS661c, which was used as a mucosal challenge virus in this study, is a highly pathogenic molecular clone of a variant of SHIV-89.6 possessing a tropism of CXCR-4. In our preliminary study, the SHIV virus infected GHOST-X4 cells in vitro and the virus challenge eliminated the naïve $CD4^+$ T-cell population in the peripheral blood in macaques, findings which confirmed those by Nishimura et al. (33, 34). In conjunction with CCR5-tropic pathogenic SIVsmE660, Ourmanov et al. obtained similar results with the partial control of homologous viremia by the recombinant MVA vaccination (35). Furthermore, the potential of the DNA vaccination to induce a broad spectrum of mucosal protection against heterologous SIV/DeltaB670 has been demonstrated (13).

Although the virus-specific immune elicitation by DNA/Ad5 vaccination was extremely high in immunized animals (45), the efficacy results for a DNA/Ad5 study with an SIVmac239 were not comparable to those for SHIV 89.6 (43). These discrepancies in vaccine efficacy by challenge viruses suggest that SIVmac239 might be a difficult virus to control by the active immunization of various vaccine candidates. Since DNA/Ad5 is expected to elicit higher levels of immunity than either MVA or DNA alone (43–45), it might be possible to obtain vaccine efficacy in conjunction with different CCR5-tropic SIV or SHIV from SIVmac239. Alternatively, a multicomponent DNA/Ad5 might elicit broad-spectrum immunity as well as protection against SIV or CCR5-SHIV. Recently, a DNA/Sendai virus vaccination (27) proved to be as effective at controlling SIVmac239 as an attenuated live SIV vaccine (10, 11), opening the possibility for studies comparing the protective immunity elicited by ordinary vaccination to that induced by attenuated live SIV vaccination.

Because the lack of an exact HIV-1 macaque model significantly limits our ability to study and calibrate vaccine efficacy, we may need to rely on parameters such as the control of viremia, the loss of $CD4^+$ cells, and the absence of mortality to establish the efficacy of a tested vaccine against an immunodeficiency virus. Certainly, such parameters would represent a more realistic goal for the development of a preventive vaccine in the macaque model. They may also play a key role in the evaluation of vaccine efficacy in human trials I/II using the vaccine modalities developed in the macaque model.

It was recently reported that the AIDS vaccine failed in rhesus macaques approximately six months post-virus challenge, with viral avoidance of cytotoxic T-lymphocyte recognition posing a major limitation to cytotoxic T-lymphocyte-based AIDS vaccines (4). In contrast, the rBCG/rDIs prime-boost vaccine was shown in this study to control viral load throughout the 1-year observation period, suggesting that it may improve the prospects for a vaccine regimen capable of providing long-term protection against HIV-1 replication and disease progression (38, 49). Work is under way to determine whether this rBCG/rDIs vaccine will fail to control the plasma viral load in the macaque model, a failure associated with the viral escape of antigen-specific cytotoxic T lymphocytes.

The route of recombinant DIs administration will be key to effectively inducing immunity in humans. In the preliminary study to determine cellular immune induction, hundred times more rDIs was needed to achieve SIV Gag antigen-specific immunity in macaques by the intradermal (10^8 PFU/ml) than by the intravenous (10^6 PFU/ml) route (K. Someya et al., unpublished data). These findings may suggest that replication-defective vaccinia virus DIs is effective at eliciting antigen-specific immunity by intravenous administration. In addition, they suggest that the intravenous inoculation of rDIs may more effectively induce specific immunity than intradermal inoculation, although intravenous inoculation is not practical for use in human.

This study did not show a clear correlation between levels of virus-specific cellular immunity induced by booster inoculations with rDIs to rBCG-primed animals and protection against a highly virulent immunodeficiency virus after mucosal challenge. The levels of both virus-specific IFN-γ ELISPOT and gamma interferon cytokine staining responses in peripheral blood from animals in the rBCG/rDIs group were the highest of the five groups studied. Why did the prime-boost vaccination of animals of the rBCG/rDIs group prove more effective than the vaccine protocols used with the other groups? We speculate that rBCG priming, which occurs at the skin region of the thigh near the inguinal and iliac lymph nodes

draining the genitorectal mucosa, may elicit mucosal immunity in the region (23). Furthermore, we showed that the two booster intravenous inoculations with rDIs help induce a level of protective immunity sufficient to control a mucosal viral challenge in the immunized animals. Although the two intravenous inoculations with rDIsSIVgag alone proved capable of inducing some virus-specific immunity in peripheral blood after the homologous booster immunization in the immunized animals (DIs group), they appeared to provide no protection against the mucosal viral challenge.

The *M. bovis* BCG/DIs prime-boost vaccination might thus provide the opportunity to study the relationship between protection against mucosal viral challenge and elicitation of systemic or mucosal immunity. Our findings regarding the efficacy of the *M. bovis* BCG/DIs prime-boost vaccine regimen confirm those by Lehner et al. (23) and they further demonstrated a significant association between protection from mucosal rectal infection with SIV and an increase in the levels of CD8 suppressor factor and beta-chemokine. Although we cannot fully explain the differences in vaccine efficacy at this moment, it is likely that the routes of immunization and of challenge, the character of the vaccine vectors and the immunization schedule all play profound roles in eliciting vaccine efficacy in macaques.

Recently, considerable progress has been made in understanding *M. bovis* BCG as a HIV vaccine vector. Our own group demonstrated that recombinant *M. bovis* BCG vectors have the potential to deliver an HIV immunogen for desirable immune elicitation in macaques (46). Furthermore, *M. bovis* BCG vaccine substrain Tokyo 172 was revealed to be avirulent in HIV-infected children (16). The insertion of a full-length SIVmac239 *gag* into the *M. bovis* BCG substrain Tokyo 172 does not affect its toxicity, stability, or efficacy against *Mycobacterium tuberculosis* (54). Furthermore, rBCG has been shown to be nonvirulent in immunodeficient mice (54). These findings highlight the utility of rBCG as a vector for HIV-1 vaccine development.

In summary, our results demonstrate that a prime-boost vaccine regimen using rBCG as the prime and vaccinia virus rDIs as the boost can induce effective immunity against a mucosal infection with a highly virulent immunodeficiency virus for at least a year. Both of the vectors are safe for humans, making them attractive candidates for use in a preventive prime-boost vaccine against HIV-1.

ACKNOWLEDGMENTS

We thank David I. Watkins, Wisconsin Regional Primate Center, Madison, WI; Jorge Flores, Bernard Moss, Bonnie Mathieson, and Rebecca Sheets, National Institute of Allergy and Infectious Diseases, National Institutes of Health, Bethesda, MD, and Vijay Mehra and Patricia Fast from the International AIDS Vaccine Initiative, New York, NY, for their helpful comments. We also thank Tadashi Nakasone, AIDS Research Center, National Institute of Infectious Diseases, for the quantitative analysis of plasma viral loads and for his helpful comments.

This work was supported by the Panel on AIDS of the U.S.-Japan Cooperative Medical Science Program, the Human Science Foundation, Japan, and the Japanese Ministry of Health, Labor and Welfare. This study was also supported by the AIDS vaccine project of the Japan Science and Technology Agency (JST).

REFERENCES

1. **Aldovini, A., and R. A. Young.** 1991. Humoral and cell-mediated immune responses to live recombinant BCG-HIV vaccines. Nature 351:479–482.
2. **Amara, R. R., and H. L. Robinson.** 2002. A new generation of HIV vaccines. Trends Mol. Med. 8:489–495.
3. **Amara, R. R., F. Villinger, J. D. Altman, S. L. Lydy, S. P. O'Neil, S. I. Staprans, D. C. Montefiori, Y. Xu, J. G. Herndon, L. S. Wyatt, M. A. Candido, N. L. Kozyr, P. L. Earl, J. M. Smith, H. L. Ma, B. D. Grimm, M. L. Hulsey, J. Miller, H. M. McClure, J. M. McNicholl, B. Moss, and H. L. Robinson.** 2001. Control of a mucosal challenge and prevention of AIDS by a multiprotein DNA/MVA vaccine. Science 292:69–74.
4. **Barouch, D. H., J. Kunstman, M. J. Kuroda, J. E. Schmitz, S. Santra, F. W. Peyerl, G. R. Krivulka, K. Beaudry, M. A. Lifton, D. A. Gorgone, D. C. Montefiori, M. G. Lewis, S. M. Wolinsky, and N. L. Letvin.** 2002. Eventual AIDS vaccine failure in a rhesus monkey by viral escape from cytotoxic T lymphocytes. Nature 415:335–339.
5. **Barouch, D. H., S. Santra, J. E. Schmitz, M. J. Kuroda, T. M. Fu, W. Wagner, M. Bilska, A. Craiu, X. X. Zheng, G. R. Krivulka, K. Beaudry, M. A. Lifton, C. E. Nickerson, W. L. Trigona, K. Punt, D. C. Freed, L. Guan, S. Dubey, D. Casimiro, A. Simon, M. E. Davies, M. Chastain, T. B. Strom, R. S. Gelman, D. C. Montefiori, M. G. Lewis, E. A. Emini, J. W. Shiver, and N. L. Letvin.** 2000. Control of viremia and prevention of clinical AIDS in rhesus monkeys by cytokine-augmented DNA vaccination. Science 290:486–492.
6. **Chaparas, S. D., and S. R. Hedrick.** 1973. Comparison of strains of BCG. I. Antigenic analysis and tuberculin reactivity. Infect. Immun. 7:777–780.
7. **Chujoh, Y., K. Matsuo, H. Yoshizaki, T. Nakasatomi, K. Someya, Y. Okamoto, S. Naganawa, S. Haga, H. Yoshikura, A. Yamazaki, S. Yamazaki, and M. Honda.** 2001. Cross-clade neutralizing antibody production against human immunodeficiency virus type 1 clade E and B' strains by recombinant *Mycobacterium bovis* BCG-based candidate vaccine. Vaccine 20:797–804.
8. **Daniel, M. D., F. Kirchhoff, S. C. Czajak, P. K. Sehgal, and R. C. Desrosiers.** 1992. Protective effects of a live attenuated SIV vaccine with a deletion in the nef gene. Science 258:1938–1941.
9. **Davis, N. L., A. West, E. Reap, G. MacDonald, M. Collier, S. Dryga, M. Maughan, M. Connell, C. Walker, K. McGrath, C. Cecil, L. H. Ping, J. Frelinger, R. Olmsted, P. Keith, R. Swanstrom, C. Williamson, P. Johnson, D. Montefiori, and R. E. Johnston.** 2002. Alphavirus replicon particles as candidate HIV vaccines. IUBMB Life 53:209–211.
10. **Desrosiers, R. C.** 1992. HIV with multiple gene deletions as a live attenuated vaccine for AIDS. AIDS Res. Hum. Retroviruses 8:1457.
11. **Desrosiers, R. C., M. S. Wyand, T. Kodama, D. J. Ringler, L. O. Arthur, P. K. Sehgal, N. L. Letvin, N. W. King, and M. D. Daniel.** 1989. Vaccine protection against simian immunodeficiency virus infection. Proc. Natl. Acad. Sci. USA 86:6353–6357.
12. **Fauci, A. S., S. M. Schnittman, G. Poli, S. Koenig, and G. Pantaleo.** 1991. NIH conference on immunopathogenic mechanisms in human immunodeficiency virus infection. Ann. Intern. Med. 114:678–693.
13. **Fuller, D. H., P. A. Rajakumar, L. A. Wilson, A. M. Trichel, J. T. Fuller, T. Shipley, M. S. Wu, K. Weis, C. R. Rinaldo, J. R. Haynes, and M. Murphey-Corb.** 2002. Induction of mucosal protection against primary, heterologous simian immunodeficiency virus by a DNA vaccine. J. Virol. 76:3309–3317.
14. **Gauduin, M. C., R. L. Glickman, S. Ahmad, T. Yilma, and R. P. Johnson.** 1999. Characterization of SIV-specific $CD4^+$ T-helper proliferative responses in macaques immunized with live-attenuated SIV. J. Med. Primatol. 28:233–241.
15. **Hel, Z., D. Venzon, M. Poudyal, W. P. Tsai, L. Giuliani, R. Woodward, C. Chougnet, G. Shearer, J. D. Altman, D. Watkins, N. Bischofberger, A. Abimiku, P. Markham, J. Tartaglia, and G. Franchini.** 2000. Viremia control following antiretroviral treatment and therapeutic immunization during primary SIV251 infection of macaques. Nat. Med. 6:1140–1146.
16. **Hesseling, A. C., H. S. Schaaf, W. A. Hanekom, N. Beyers, M. F. Cotton, R. P. Gie, B. J. Marais, P. van Helden, and R. M. Warren.** 2003. Danish bacille Calmette-Guerin vaccine-induced disease in human immunodeficiency virus-infected children. Clin. Infect. Dis. 37:1226–1233.
17. **Honda, M., K. Matsuo, T. Nakasone, Y. Okamoto, H. Yoshizaki, K. Kitamura, W. Sugiura, K. Watanabe, Y. Fukushima, S. Haga, Y. Katsura, K. Kitamura, H. Tasaka, K. Komuro, T. Yamada, T. Asano, A. Yamazaki, and S. Yamazaki.** 1995. Protective immune responses induced by secretion of a chimeric soluble protein from a recombinant *Mycobacterium bovis* bacillus Calmette-Guérin vector candidate vaccine for human immunodeficiency virus type 1 in small animals. Proc. Natl. Acad. Sci. USA 92:10693–10697.
18. **Ishii, K., Y. Ueda, K. Matsuo, Y. Matsuura, T. Kitamura, K. Kato, Y. Izumi, K. Someya, T. Ohsu, M. Honda, and T. Miyamura.** 2002. Structural analysis of vaccinia virus DIs strain: application as a new replication-deficient viral vector. Virology 302:433–444.
19. **Jacobs, W. R., Jr., M. Tuckman, and B. R. Bloom.** 1987. Introduction of foreign DNA into mycobacteria using a shuttle phasmid. Nature 327:532–535.
20. **Karacostas, V., E. J. Wolffe, K. Nagashima, M. A. Gonda, and B. Moss.** 1993. Over expression of the HIV-1 gag-pol polyprotein results in intracellular

activation of HIV-1 protease and inhibition of assembly and budding of virus-like particles. Virology 193:661–671.
21. Kawahara, M., K. Matsuo, T. Nakasone, T. Hiroi, H. Kiyono, S. Matsumoto, T. Yamada, N. Yamamoto, and M. Honda. 2002. Combined intrarectal/intradermal inoculation of recombinant *Mycobacterium bovis* bacillus Calmette-Guérin (BCG) induces enhanced immune responses against the inserted HIV-1 V3 antigen. Vaccine 21:158–166.
22. Kitamura, T., Y. Kitamura, and I. Tagaya. 1967. Immunogenicity of an attenuated strain of vaccinia virus on rabbits and monkeys. Nature 215:1187–1188.
23. Lehner, T., Y. Wang, M. Cranage, L. A. Bergmeier, E. Mitchell, L. Tao, G. Hall, M. Dennis, N. Cook, R. Brookes, L. Klavinskis, I. Jones, C. Doyle, and R. Ward. 1996. Protective mucosal immunity elicited by targeted iliac lymph node immunization with a subunit SIV envelope and core vaccine in macaques. Nat. Med. 2:767–775.
24. Letvin, N. L., D. H. Barouch, and D. C. Montefiori. 2002. Prospects for vaccine protection against HIV-1 infection and AIDS. Annu. Rev. Immunol. 20:73–99.
25. Lifson, J. D., M. Piatak, Jr., J. L. Rossio, J. Bess, Jr., E. Chertova, D. Schneider, R. Kiser, V. Coalter, B. Poore, R. Imming, R. C. Desrosiers, L. E. Henderson, and L. O. Arthur. 2002. Whole inactivated SIV virion vaccines with functional envelope glycoproteins: safety, immunogenicity, and activity against intrarectal challenge. J. Med. Primatol. 31:205–216.
26. Lu, Y., M. S. Salvato, C. D. Pauza, J. Li, J. Sodroski, K. Manson, M. Wyand, N. Letvin, S. Jenkins, N. Touzjian, C. Chutkowski, N. Kushner, M. LeFaile, L. G. Payne, and B. Roberts. 1996. Utility of SHIV for testing HIV-1 vaccine candidates in macaques. J. Acquir. Immune Defic. Syndr. Hum. Retrovirol. 12:99–106.
27. Matano, T., M. Kobayashi, H. Igarashi, A. Takeda, H. Nakamura, M. Kano, C. Sugimoto, K. Mori, A. Iida, T. Hirata, M. Hasegawa, T. Yuasa, M. Miyazawa, Y. Takahashi, M. Yasunami, A. Kimura, D. H. O'Connor, D. I. Watkins, and Y. Nagai. 2004. Cytotoxic T lymphocyte-based control of simian immunodeficiency virus replication in a preclinical AIDS vaccine trial. J. Exp. Med. 199:1709–1718.
28. Matsumoto, S., M. Tamaki, H. Yukitake, T. Matsuo, N. Mariko, H. Teraoka, and T. Yamada. 1996. A stable *Escherichia coli*-mycobacteria shuttle vector pSO246 in *Mycobacterium bovis* BCG. FEMS Microbiol. Lett. 135:237–243.
29. McMichael, A. J., and T. Hanke. 2003. HIV vaccines 1983–2003. Nat. Med. 9:874–880.
30. Mori, K., Y. Yasutomi, S. Ohgimoto, T. Nakasone, S. Takamura, T. Shioda, and Y. Nagai. 2001. Quintuple deglycosylation mutant of simian immunodeficiency virus SIVmac239 in rhesus macaques: robust primary replication, tightly contained chronic infection, and elicitation of potent immunity against the parental wild-type strain. J. Virol. 75:4023–4028.
31. Mothe, B. R., H. Horton, D. K. Carter, T. M. Allen, M. E. Liebl, P. Skinner, T. U. Vogel, S. Fuenger, K. Vielhuber, W. Rehrauer, N. Wilson, G. Franchini, J. D. Altman, A. Haase, L. J. Picker, D. B. Allison, and D. I. Watkins. 2002. Dominance of CD8 responses specific for epitopes bound by a single major histocompatibility complex class I molecule during the acute phase of viral infection. J. Virol. 76:875–884.
32. Nabel, G., W. Makgoba, and J. Esparza. 2002. HIV-1 diversity and vaccine development. Science 296:2335.
33. Nishimura, Y., C. R. Brown, J. J. Mattapallil, T. Igarashi, A. Buckler-White, B. A. Lafont, V. M. Hirsch, M. Roederer, and M. A. Martin. 2005. Resting naive CD4+ T cells are massively infected and eliminated by X4-tropic simian-human immunodeficiency viruses in macaques. Proc. Natl. Acad. Sci. USA 102:8000–8005.
34. Nishimura, Y., T. Igarashi, O. K. Donau, A. Buckler-White, C. Buckler, B. A. Lafont, R. M. Goeken, S. Goldstein, V. M. Hirsch, and M. A. Martin. 2004. Highly pathogenic SHIVs and SIVs target different CD4+ T-cell subsets in rhesus monkeys, explaining their divergent clinical courses. Proc. Natl. Acad. Sci. USA 101:12324–12329.
35. Ourmanov, I., C. R. Brown, B. Moss, M. Carroll, L. Wyatt, L. Pletneva, S. Goldstein, D. Venzon, and V. M. Hirsch. 2000. Comparative efficacy of recombinant modified vaccinia virus Ankara expressing simian immunodeficiency virus (SIV) Gag-Pol and/or Env in macaques challenged with pathogenic SIV. J. Virol. 74:2740–2751.
36. Ramsburg, E., N. F. Rose, P. A. Marx, M. Mefford, D. F. Nixon, W. J. Moretto, D. Montefiori, P. Earl, B. Moss, and J. K. Rose. 2004. Highly effective control of an AIDS virus challenge in macaques by using vesicular stomatitis virus and modified vaccinia virus Ankara vaccine vectors in a single-boost protocol. J. Virol. 78:3930–3940.
37. Reimann, K. A., J. T. Li, G. Voss, C. Lekutis, K. Tenner-Racz, P. Racz, W. Lin, D. C. Montefiori, D. E. Lee-Parritz, Y. Lu, R. G. Collman, J. Sodroski, and N. L. Letvin. 1996. An env gene derived from a primary human immunodeficiency virus type 1 isolate confers high in vivo replicative capacity to a chimeric simian/human immunodeficiency virus in rhesus monkeys. J. Virol. 70:3198–3206.
38. Ruprecht, R. M., T. W. Baba, R. Rasmussen, Y. Hu, and P. L. Sharma. 1996. Murine and simian retrovirus models: the threshold hypothesis. AIDS 10(Suppl. A):S33–40.
39. Sakai, K., K. Shinohara, E. Takahashi, Y. Izumi, Y. Ami, Y. Sasaki, T. Nakasone, and M. Honda. 2001. Molecular cloning of a pathogenic simian-human immunodeficiency virus for HIV/AIDS monkey model. Sixth International Congress on AIDS in Asia and the Pacific, 5–10 October 2001, Melbourne, Australia, abstract p. 84.
40. Sasaki, Y., Y. Ami, T. Nakasone, K. Shinohara, E. Takahashi, S. Ando, K. Someya, Y. Suzaki, and M. Honda. 2000. Induction of CD95 ligand expression on T lymphocytes and B lymphocytes and its contribution to apoptosis of CD95-up-regulated $CD4^-$ T lymphocytes in macaques by infection with a pathogenic simian/human immunodeficiency virus. Clin. Exp. Immunol. 122:381–389.
41. Sher, N. A., S. D. Chaparas, L. E. Greenberg, and S. Bernard. 1975. Effects of BCG, *Corynebacterium parvum*, and methanol extraction residue in the reduction of mortality from *Staphylococcus aureus* and *Candida albicans* infections in immunosuppressed mice. Infect. Immun. 12:1325–1330.
42. Shinohara, K., K. Sakai, S. Ando, Y. Ami, N. Yoshino, E. Takahashi, K. Someya, Y. Suzaki, T. Nakasone, Y. Sasaki, M. Kaizu, Y. Lu, and M. Honda. 1999. A highly pathogenic simian/human immunodeficiency virus with genetic changes in cynomolgus monkey. J. Gen. Virol. 80:1231–1240.
43. Shiver, J. W. 2004. Development of an HIV-1 vaccine based on replication-defective adenovirus. Proc. Keystone Symp. 2004:12.
44. Shiver, J. W., and E. A. Emini. 2004. Recent advances in the development of HIV-1 vaccines using replication-incompetent adenovirus vectors. Annu. Rev. Med. 55:355–372.
45. Shiver, J. W., T. M. Fu, L. Chen, D. R. Casimiro, M. E. Davies, R. K. Evans, Z. Q. Zhang, A. J. Simon, W. L. Trigona, S. A. Dubey, L. Huang, V. A. Harris, R. S. Long, X. Liang, L. Handt, W. A. Schleif, L. Zhu, D. C. Freed, N. V. Persaud, L. Guan, K. S. Punt, A. Tang, M. Chen, K. A. Wilson, K. B. Collins, G. J. Heidecker, V. R. Fernandez, H. C. Perry, J. G. Joyce, K. M. Grimm, J. C. Cook, P. M. Keller, D. S. Kresock, H. Mach, R. D. Troutman, L. A. Isopi, D. M. Williams, Z. Xu, K. E. Bohannon, D. B. Volkin, D. C. Montefiori, A. Miura, G. R. Krivulka, M. A. Lifton, M. J. Kuroda, J. E. Schmitz, N. L. Letvin, M. J. Caulfield, A. J. Bett, R. Youil, D. C. Kaslow, and E. A. Emini. 2002. Replication-incompetent adenoviral vaccine vector elicits effective anti-immunodeficiency-virus immunity. Nature 415:331–335.
46. Someya, K., D. Cecilia, Y. Ami, T. Nakasone, K. Matsuo, S. Burda, H. Yamamoto, N. Yoshino, M. Kaizu, S. Ando, K. Okuda, S. Zolla-Pazner, S. Yamazaki, N. Yamamoto, and M. Honda. 2005. Vaccination of rhesus macaques with recombinant *Mycobacterium bovis* bacillus Calmette-Guérin Env V3 elicits neutralizing antibody-mediated protection against simian-human immunodeficiency virus with a homologous but not a heterologous V3 motif. J. Virol. 79:1452–1462.
47. Someya, K., K. Q. Xin, K. Matsuo, K. Okuda, N. Yamamoto, and M. Honda. 2004. A consecutive priming-boosting vaccination of mice with simian immunodeficiency virus (SIV) *gag/pol* DNA and recombinant vaccinia virus strain DIs elicits effective anti-SIV immunity. J. Virol. 78:9842–9853.
48. Stover, C. K., V. F. de la Cruz, T. R. Fuerst, J. E. Burlein, L. A. Benson, L. T. Bennett, G. P. Bansal, J. F. Young, M. H. Lee, G. F. Hatfull, S. B. Snapper, R. G. Barletta, W. R. Jacobs, and B. R. Bloom. 1991. New use of BCG for recombinant vaccines. Nature 351:456–460.
49. Strathdee, S. A., K. J. Craib, R. S. Hogg, M. V. O'Shaughnessy, J. S. Montaner, and M. T. Schechter. 1995. Long-term non-progression in HIV infection. Lancet 346:1372.
50. Tagaya, I., T. Kitamura, and Y. Sano. 1961. A new mutant of dermovaccinia virus. Nature 192:381–382.
51. Takeya, K., K. Nomoto, S. Murasoka, S. Shimotori, T. Taniguchi, and T. Miyake. 1977. Growth of two strains of *Mycobacterium bovis* (BCG) in a thymic mice. J. Gen. Microbiol. 100:403–405.
52. Thole, J. E., W. J. Keulen, J. De Bruyn, A. H. Kolk, D. G. Groothuis, L. G. Berwald, R.H. Tiesjema, and J. D. van Embden. 1987. Characterization, sequence determination, and immunogenicity of a 64-kilodalton protein of *Mycobacterium bovis* BCG expressed in *Escherichia coli* K-12. Infect. Immun. 55:1466–1475.
53. Ueda, K., S. Yamazaki, J. Saegusa, and S. Someya. 1978. Progressive and fetal infection with attenuated *Mycobacterium bovis* (BCG) in nude mice. Jpn. J. Exp. Med. 48:533–543.
54. Yamamoto, S., T. Yamamoto, S. Haga, and M. Honda. 2003. Presented at the Tuberculosis Leprosy Research Conference U.S.-Japan Co. Med. Sci.
55. Yoshino, N., Y. Ami, K. Terao, F. Tashiro, and M. Honda. 2000. Upgrading of flow cytometric analysis for absolute counts, cytokines and other antigenic molecules of cynomolgus monkeys (*Macaca fascicularis*) by using anti-human cross-reactive antibodies. Exp. Anim. 49:97–110.

INFECTION AND IMMUNITY, Oct. 2005, p. 6892–6902
0019-9567/05/$08.00+0 doi:10.1128/IAI.73.10.6892–6902.2005

Vol. 73, No. 10

Enterotoxin-Based Mucosal Adjuvants Alter Antigen Trafficking and Induce Inflammatory Responses in the Nasal Tract

Frederik W. van Ginkel,[1,2]* Raymond J. Jackson,[2] Naoto Yoshino,[2] Yukari Hagiwara,[2] Daniel J. Metzger,[3] Terry D. Connell,[3] Hong L. Vu,[2] Michael Martin,[2] Kohtaro Fujihashi,[2] and Jerry R. McGhee[2]

Department of Pathobiology, College of Veterinary Medicine, Auburn University, Auburn, Alabama 36849[1]; Departments of Microbiology and Pediatric Dentistry, University of Alabama at Birmingham, Birmingham, Alabama 35294-2170[2]; and Departments of Microbiology and Oral Biology, School of Medicine and Biomedical Sciences, State University of New York at Buffalo, Buffalo, New York 14214[3]

Received 8 February 2005/Returned for modification 18 March 2005/Accepted 25 May 2005

The safety of nasal vaccines containing enterotoxin-based mucosal adjuvants has not been studied in detail. Previous studies have indicated that native cholera toxin (nCT) can alter antigen trafficking when applied nasally. In this study, we determined the enterotoxin-based variables that alter antigen trafficking. To measure the influence of enterotoxin-based mucosal adjuvants on antigen trafficking in the nasal tract, native and mutant enterotoxins were coadministered with radiolabeled tetanus toxoid (TT). The nCT and heat-labile enterotoxin type 1 (LTh-1) redirected TT into the olfactory neuroepithelium (ON/E). Antigen redirection occurred mainly across the nasal epithelium without subsequent transport along olfactory neurons into the olfactory bulbs (OB). Thus, no significant accumulation of the vaccine antigen TT was observed in the OB when coadministered with nCT. In contrast, neither mutant CT nor mutant LTh-1, which lack ADP-ribosyltransferase activity, redirected TT antigen into the ON/E. Thus, ADP-ribosyltransferase activity was essential for antigen trafficking across the olfactory epithelium. Accumulation of TT in the ON/E was also due to B-subunit binding to GM1 gangliosides, as was demonstrated (i) by redirection of TT by LTh-1 in a dose-dependent manner, (ii) by ganglioside inhibition of the antigen redirection by LTh-1 and nCT, and (iii) by the use of LT-IIb, a toxin that binds to gangliosides other than GM1. Redirection of TT into the ON/E coincided with elevated production of interleukin 6 (IL-6) but not IL-1β or tumor necrosis factor alpha in the nasal mucosa. Thus, redirection of TT is dependent on ADP-ribosyltransferase activity and GM1 binding and is associated with production of the inflammatory cytokine IL-6.

Enterotoxins are powerful mucosal adjuvants; however, the mechanisms for their adjuvanticity are still being defined. Native cholera toxin (nCT) and the *Escherichia coli*-derived heat-labile toxin (human type 1) (nLTh-1) are both potent mucosal adjuvants for coadministered protein antigens when given by the oral, nasal, or parenteral route (4, 9–11, 33, 42, 50). Despite extensive research on these enterotoxins, mucosal adjuvants for human use remain in experimental phases, and recent studies have focused on generating nontoxic mutants of CT (mCT) and LTh-1 (mLTh-1). Detoxification of these enterotoxins was accomplished by site-directed mutagenesis of the ADP-ribosylation site located in the A subunit of these AB_5 enterotoxins (3, 8, 51, 52, 53, 54). These mutants are effective mucosal adjuvants in mice and induce long-term memory for coadministered proteins given either by the nasal or parenteral route (3, 51, 52). In this regard, the nasal route is perhaps superior to oral delivery, since it requires much lower doses of both adjuvant and coadministered proteins/vaccines.

Both nCT and nLTh-1 are part of serogroup I of the heat-labile enterotoxins (38) and display somewhat different ganglioside binding specificities (12). For example, nCT binds predominantly to GM1, while nLTh-1 preferentially binds to GM1 and to a lesser extent to GD1b and binds weakly to GM2 and asialo-GM1 (12). Native LTh-I not only targets gangliosides, but also binds to other glycoproteins in the intestinal tract and is associated with a much larger repertoire of target molecules than has been reported for CT (18, 25). The heat-labile enterotoxins from serogroup II, such as LT-IIb, display different ganglioside binding specificities. LT-IIb binds to GD1a and to a lesser extent to GT1b and showed no affinity for GM1 (12). LT-IIb functioned as a mucosal adjuvant when given nasally and induced a mucosal immune response consistent with a mixed $CD4^+$ Th1/Th2 cell response (34), as was previously reported for nLTh-1 (42). A lack of ganglioside binding, which was accomplished by site-directed mutagenesis of amino acid 33, the G33D mutation, rendered both nCT and nLTh-1 deficient in GM1 binding and in the ability to function as mucosal adjuvants following oral (21) or nasal (7) application. Enterotoxin binding to gangliosides is functionally important for both mucosal adjuvanticity and enterotoxicity. Both nCT and nLTh-1 bind to GM1 on epithelial cells and are endocytosed and transported. Blocking GM1 sites is not sufficient to ameliorate the enterotoxicity of nLTh-1, since the molecule also binds to other intestinal epithelial glycoproteins (26, 55).

ADP-ribosyltransferase activity in nCT may potentially cause damage due to toxicity and inflammation of the nasal epithelium, and in so doing may allow passive entry of co-delivered vaccine proteins into the olfactory nerve/epithelium (ON/E) (14). Increased permeability of the gut epithelium for

* Corresponding author. Mailing address: Department of Pathobiology, College of Veterinary Medicine, Auburn University, 217 Scott Ritchey, Auburn, AL 36849. Phone: (334) 844-0132. Fax: (334) 844-2652. E-mail: vangifw@vetmed.auburn.edu.

low-molecular-weight dextran was seen when nCT was orally administered. This study suggested that increased permeability may be an intricate part of the ability of nCT to function as a mucosal adjuvant (32). This conclusion was supported by the fact that CT-B, which is a poor oral adjuvant, did not cause permeability changes in the gut epithelium (32).

The hypothesis proposed in this study was that part of the adjuvanticity of enterotoxin-based mucosal adjuvants may reflect their ability to alter antigen trafficking in the nasal tract and that this antigen redirection could contribute to enhanced inflammatory reactions, which may differentially boost mucosal immune responses.

In this study, we show that enterotoxin-based mucosal adjuvants, i.e., nCT and nLTh-1, alter codelivered protein vaccine trafficking into the ON/E when given nasally. This process of antigen redirection requires ADP-ribosyltransferase activity of the enterotoxin-based adjuvant, as well as binding to GM1 gangliosides, and coincided with the production of the inflammatory cytokine interleukin 6 (IL-6). On the other hand, mutants of CT and LTh-1 lacking ADP-ribosyltransferase activity did not redirect antigen into the ON/E, nor did the native toxin LT-IIb, which is not able to bind GM1. In conclusion, both ADP-ribosyltransferase activity and GM1 binding are required in order for enterotoxin to redirect antigen into the ON/E.

MATERIALS AND METHODS

Mice. Mice of the C57BL/6 strain 6 to 7 weeks of age were obtained from Charles River Laboratories (Wilmington, MA). The mice were maintained in horizontal laminar flow cabinets and were pathogen free as determined by plasma antibody screening and tissue histopathology performed on sentinel mice. All mice received sterile food and water ad libitum and were between 8 and 12 weeks of age when used for these experiments. All mouse studies were done in accordance with guidelines of both the NIH and the Animal Institutional Care and Use Committee of the University of Alabama at Birmingham to avoid pain and distress.

Enterotoxin production and purification. The enterotoxins were produced in our laboratory, with the exception of nCT, which was purchased (List Biological Laboratories, Inc., Campbell, CA). The mCT (E112K) was generated by site-directed mutagenesis of single-stranded DNA of *Escherichia coli* CJ236 transfected with M13 mp19, which included the CT gene, using the Mutant K system (Takara Biomedicals, Kyoto, Japan) as described previously (29, 53). The glutamate-to-lysine mutation of amino acid 112 was generated using the 5′-GATG AACAAAAAGTTTCTGCT-3′ oligonucleotide (53). The pUC119 plasmid carrying the mutated CT gene was transformed into *E. coli* DH5α. The *E. coli* strains containing the mCT gene were grown in LB broth (10 g NaCl, 10 g tryptone, and 5 g yeast extract/liter) with 100 μg/ml of ampicillin. The resulting mCT, derived from a sonicated cell suspension, was purified by binding to and elution from a D-galactose-immobilized column (Pierce Chemical Co., Rockford, IL).

The enterotoxin gene containing plasmid pMY1900 from *E. coli* strain 1032 was subcloned by PCR into the expression vector pTrc 99A (Amersham Pharmacia Biotech, Piscataway, NJ). The LTh-1 mutant E112K was constructed by site-directed mutagenesis with specific primers as described previously (43, 44). The mLT (E112K) and LTh-1 were purified from sonicated cell suspensions and resuspended in 0.9% NaCl in 10 mM Tris-HCl buffer, pH 8.6. After centrifugation, the supernatant was subjected to a 65% ammonium sulfate precipitation, resuspended in 0.2 M Tris (pH 8.0)–1 M sucrose–10 mM EDTA (TEAN) buffer, and purified on an immobilized D-galactose column (Pierce Chemical Co.) as reported previously (45).

Heat-labile enterotoxin IIb (LT-IIb) was produced with plasmid pTDC101-transformed *E. coli* XL-1 Blue (Stratagene, La Jolla, CA) (5). The recombinant *E. coli* was grown at 37°C with vigorous shaking (225 rpm) in Luria broth (Difco Laboratories, Detroit, MI) supplemented with ampicillin (150 μg/ml; Sigma-Aldrich, St. Louis, MO) in the presence of kanamycin (50 μg/ml; Sigma-Aldrich). The expression of LT-IIb was induced during mid-log phase by the addition of 1 mM isopropyl-β-D-thiogalactoside (Sigma-Aldrich). After 4 h of growth, the bacteria were harvested by centrifugation at 8,000 × *g* for 15 min and resuspended in ice-cold 100 mM Tris-HCl (pH 8.0) containing 20% sucrose, 5 mM EDTA, polymyxin B (100 μg/ml; Sigma-Aldrich), and lysozyme (0.5 mg/ml; Sigma-Aldrich) to release the periplasm content. The supernatants were harvested after 30 min of incubation at 4°C and precipitated by 60% ammonium sulfate saturation. The precipitate was dissolved in 10 mM Tris-HCl (pH 8.0) containing 0.3 M NaCl and filter sterilized prior to gel filtration on a Sephacryl-100 column (Amersham Pharmacia Biotech), followed by chromatography with an anion-exchange Mono Q column (Amersham Pharmacia Biotech). The LT-IIb preparations were analyzed for endotoxin content with the *Limulus* amoebocyte lysate assay kit (BioWhittaker, Inc., Walkersville, MD) using an *E. coli* K235 lipopolysaccharide standard.

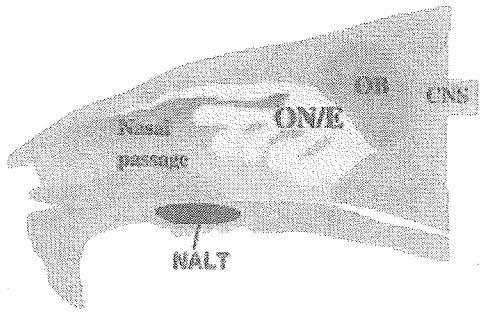

FIG. 1. Anatomy of the murine nasal tract and CNS. Indicated are the locations of the the ON/E, the NALT, and the OB in the nasal tract and adjacent CNS.

Radioiodination of proteins. Tetanus toxoid (TT) (kindly supplied by the Biken Institute, Osaka, Japan) was radiolabeled with ^{125}I. The radioiodination was performed with iodobeads (Pierce Chemicals) for 10 to 12 min at room temperature as described previously (46). Free, unincorporated ^{125}I was removed by dialysis using a Slide Dialyzer (Pierce Chemicals). The trichloroacetic acid-precipitable fraction of ^{125}I-labeled TT was used for all experiments described here. The specific activities of the radiolabeled proteins were 24.5 to 65 cpm/ng. A bicinchoninic acid protein assay (Pierce Chemicals) was used to determine the concentrations of radiolabeled proteins.

Nasal immunization. To assess the ability of ^{125}I-TT to target the ON/E following nasal application, a total of 20 μg of TT (~0.5×10^6 to 1.3×10^6 cpm) was administered in a 10-μl volume, i.e., 5 μl per nare, to naive mice. A total amount of 20 μg of ^{125}I-TT was given either alone or with the indicated enterotoxin delivered in the same volume as antigen alone. For the enterotoxins, we used 1 μg nCT, 10 μg mCT, and 10 μg mLTh-1, and for LTh-1, various amounts of protein were used, i.e., between 1 and 10 μg. For nasal application of the LTII-b enterotoxin, we used 5 μg of protein with ^{125}I-TT.

Trafficking of radiolabeled TT. We used radiolabeled TT protein to track its presence in both lymphoid and central nervous system (CNS) tissues. In these studies, ^{125}I-labeled-TT was given nasally. At 3, 6, 12, 24, and 48 h and 6 days, the ^{125}I-TT levels present in various lymphoid and CNS tissues were determined. For lymphoid tissues, the nasopharyngeal-associated lymphoreticular tissues (NALT), the cervical lymph nodes (CLNs), the mesenteric lymph nodes, the spleen, and blood (50 μl) were assessed. The isolation of NALT was performed as previously reported (49). For the CNS, we examined the ON/E, the olfactory bulbs (OB), and the remainder of the brain. These tissues were isolated as previously described (46). The radiolabeled TT in each tissue was quantitated by use of a gamma counter. The different nasal tract tissues isolated in this study are illustrated in Fig. 1.

In order to assess the influence of blocking the GM1 binding site of LTh-1 or nCT with subsequent tissue distribution of coadministered ^{125}I-TT after nasal application, the LTh-I and nCT were preincubated with a 15-fold molar excess of GM1 (Sigma-Aldrich) for 30 min at 25°C prior to nasal application. The cpm associated with different tissues 12 h after application were analyzed and compared with application without preincubation with GM1. A total of 20 μg of ^{125}I-TT and 5 μg of LTh-1 or 1 μg nCT either with or without preincubation with free GM1 was nasally administered to individual mice.

Sample collection. Blood was collected into heparinized collection tubes by retro-orbital bleeding of anesthetized mice. The plasma was separated from the cells by a 10-min centrifugation step at 10,000 × *g*. Nasal washes were collected by intubation of the trachea to access the nasopharyngeal cavity. This approach was used to avoid any blood contamination of the nasal washes. A total of 200 μl of phosphate-buffered saline (PBS) was inserted into the nasal cavity, and the